IN-SPACE TECHNOLOGY EXPERIMENTS PROGRAM

FINAL REPORT

P.52

A High Efficiency Thermal Interface (Using Condensation Heat Transfer) Between a Two-Phase Fluid Loop and Heatpipe Radiator

Experiment Definition Phase

J. A. Pohner
B. P. Dempsey
L. M. Herold

Contract No. NAS5-30357
TRW Report No. P331.LM1.90.185
TRW Sales No. 50168

JULY 1990

Prepared for:
NASA/Goddard Space Flight Center
Greenbelt, MD 20771

NASA

Report Documentation Page

1. Report No.	2. Government Accession No.	3. Recipient's Catalog No.

4. Title and Subtitle

A High Efficiency Thermal Interface (Using Condensation Heat Transfer) Between a Two-Phase Fluid Loop and a Heat Pipe Radiator

5. Report Date

July 1990

6. Performing Organization Code

7. Author(s)

John Pohner
Brian Dempsey
LeRoy Herold

8. Performing Organization Report No.

10. Work Unit No.

9. Performing Organization Name and Address

TRW Space & Technology Group
One Space Park
Redondo Beach, CA 90278

11. Contract or Grant No.

NAS5-30357

13. Type of Report and Period Covered

Final Report

12. Sponsoring Agency Name and Address

NASA/Goddard Space Flight Center
Financial Management Division
Greenbelt, MD 20771

14. Sponsoring Agency Code

15. Supplementary Notes

16. Abstract

Space Station elements and advanced military spacecraft will require rejection of tens of kilowatts of waste heat. Large space radiators and two-phase heat transport loops will be required. To minimize radiator size and weight, it is critical to minimize the temperature drop between the heat source and sink.

Under an Air Force contract, TRW developed a unique, high-performance heat exchanger for coupling the radiator to the transport loop. Since fluid flow through the heat exchanger is driven by capillary forces which are easily dominated by gravity forces in ground testing, it is necessary to perform microgravity thermal testing to verify the design.

This contract consists of an experiment definition phase leading to a preliminary design and cost estimate for a shuttle-based flight experiment of this heat exchanger design. This program will utilize modified hardware from a ground test program for the heat exchanger.

17. Key Words (Suggested by Author(s))

Heat Pipe
Gregorig Groove
Condensation
Two-Phase Fluid Loop
Spacecraft Thermal Control

18. Distribution Statement

Unclassified - Unlimited

19. Security Classif. (of this report)	20. Security Classif. (of this page)	21. No. of pages	22. Price
Unclassified	Unclassified	46	

NASA FORM 1626 OCT 86

TABLE OF CONTENTS

TABLE OF CONTENTS (continued)

LIST OF ILLUSTRATIONS

1. EXPERIMENT BACKGROUND

The High Efficiency Thermal Interface (HETI) is an efficient means for thermally coupling a two-phase coolant loop for a spacecraft to a heatpipe radiator. This section provides background information describing application of this component, theory of operation, and HETI development activities to date. The discussion which follows assumes that the two-phase coolant loop used to transport heat to the radiator is a capillary pumped loop (CPL).

1.1 Introduction

Spacecraft with small heat dissipations (less than 2 kW) have been able to reject this heat to space by conducting the payload-dissipated heat through the spacecraft structure and radiating it to space. As power levels increase and/or heat dissipating components must be located remotely from radiators, heatpipes are utilized for heat transport and isothermalization of body-mounted radiator panels. As power levels meet and exceed the 5 kW level, deployed radiators are required to provide additional radiating area since sufficient surface area may not be available on the spacecraft body. As the distance between heat dissipating payloads and radiators increase, heatpipes may no longer suffice for heat transport and pumped fluid loops may be required (see Reference [1]).

1.1-1 Effect of Temperature Drops on Radiator Area

In principle, the total thermal control system, from heat sources to radiator, could be coupled by a single fluid loop; i.e., a working fluid would be heated at the payload baseplates and would be cooled in passages distributed along the radiator panel. This configuration, however, would be very vulnerable to failure from a single micrometeoroid penetration anywhere along the extensive length of the condenser passages. For this reason, the total system is usually divided into two subsystems - the heat transport system and the heat rejection system (see Figure 1-1). The interface between the two may consist of a condenser plate for the heat transport loop which is coupled to the radiator heatpipes through a system of saddles.

One disadvantage of this two-subsystem approach is the temperature drop which results when the total heat load is transferred between the transport and rejection systems. Every degree of temperature drop translates into a increase in total radiator area required to dissipate a given heat load. In its simplest formulation, the required radiator area is given by:

$$A = \dot{Q}/[\sigma\epsilon(T^4 - T_s^4)]$$

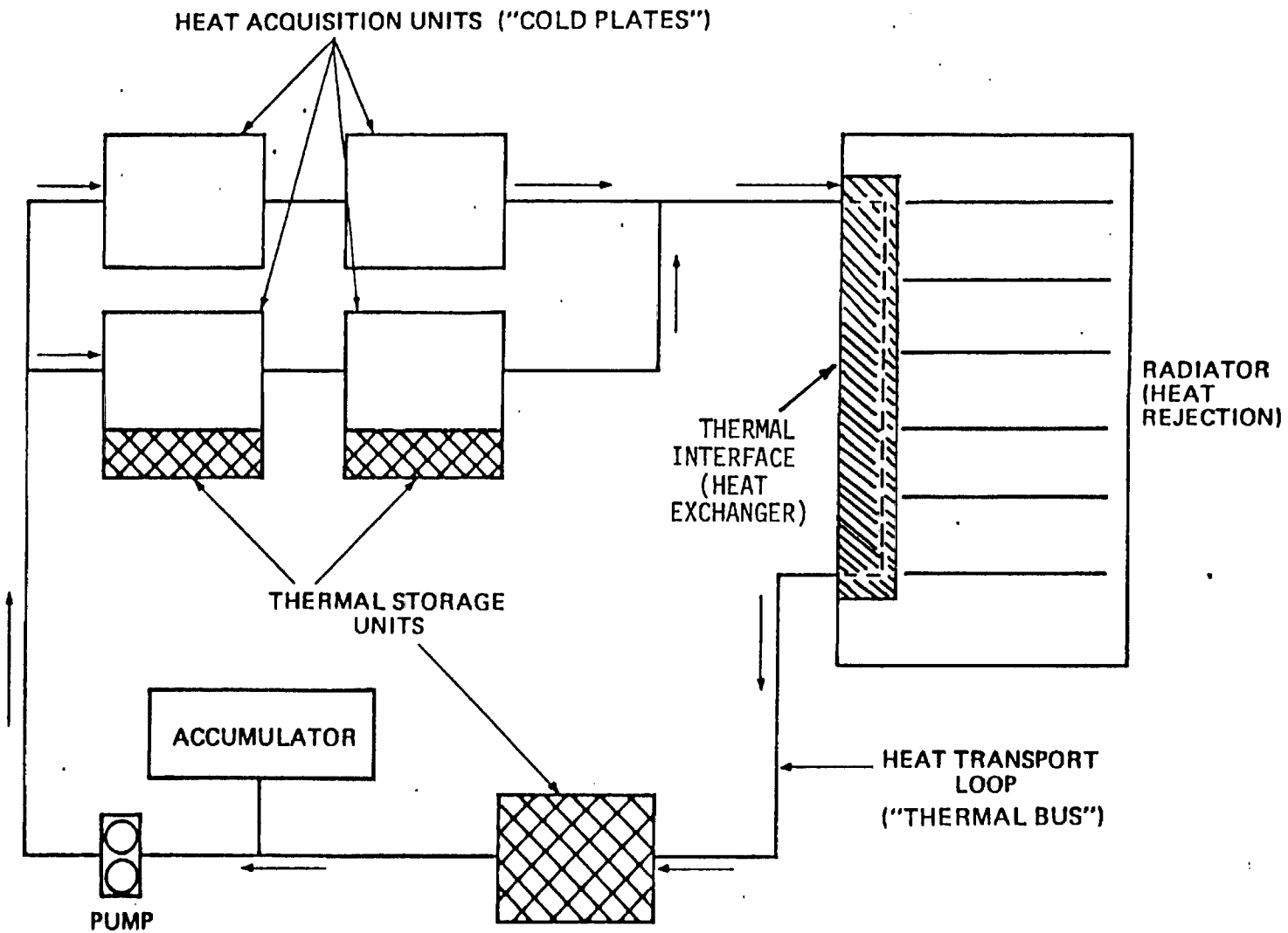

Figure 1-1. Generic Components of a High Power Spacecraft Thermal Management System

where

$\dot{Q}$ = total heat load,

ϵ = effective emissivity of the radiator,

σ = Stefan-Boltzman constant,

T = radiator temperature, and

T_S = radiative sink temperature.

The penalty resulting from a temperature drop can be measured by the radiator "area-increase factor", which is the ratio of the required radiator area to an area in the ideal case where the interface temperature drop is zero:

$$\text{area-increase factor} = [T^4 - T_S^4]/[(T-dT)^4-T_S^4]$$

where dT is the interfacial temperature drop.

Figure 1-2 gives the area-increase factor resulting from a temperature drop between the subsystems. An estimate of the radiative sink temperature as a function of orbit altitude, radiator orientation, and sun incidence angle may be found in Figure 1-3. The area-increase factor becomes larger in low earth orbits where albedo and earth infrared emission produce substantial heat loadings on the radiator and can raise the effective sink temperature to 220°K. The interface temperature drop is often substantial since a large amount of heat must be transferred through a relatively small area. It is shown in Reference [1] that the radiator weight often comprises half to three-quarters of the thermal control system weight in a high power spacecraft, so minimization of the radiator size and weight is of paramount importance.

1.1-2 Advantages of Two-Phase Heat Transport Loops

Fluid loops for cooling of spacecraft payloads may be of the (electromechanically) pumped liquid type or (electromechanically or capillary) pumped two-phase type. A pumped liquid loop is one component of the STS Orbiter thermal control system and has operated satisfactorily to date. Pump reliability, which was once the prevalent drawback of pumped liquid systems, is no longer the major design concern since extensive life testing of these pumps has shown that five year operational lifetimes are attainable. One important drawback of pumped liquid loops is the lack of isothermality throughout the circuit since heat addition or removal results in a sensible heat change of the working fluid. Thus, payloads near the inlet of a cold plate may be considerably cooler than payloads near the outlet of the same cold plate. A greater degree of isothermality may be achieved by increasing the liquid mass flowrate (and pumping power required), but a pumped liquid loop cannot approach

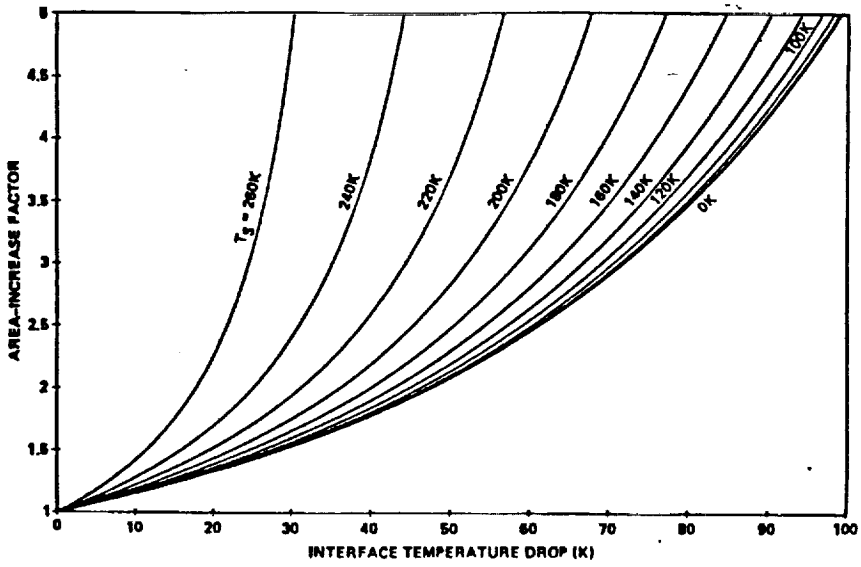

Figure 1-2. Required Increase in Radiator Area Resulting from a Subsystem Interface Temperature Drop dT for a Radiative Sink Temperature T_S and 300 K Radiator

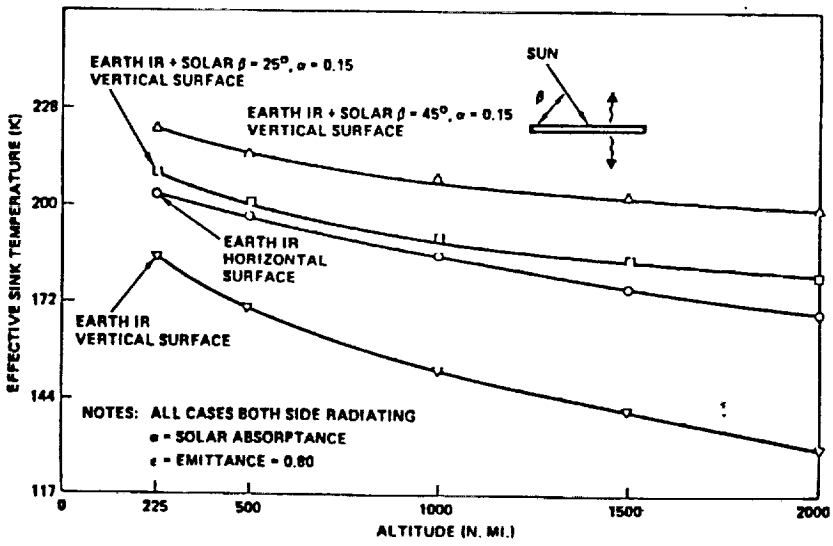

Figure 1-3. Estimate of Radiative Sink Temperature as a Function of Orbit Altitude, Radiator Orientation, and Sun Incidence Angle

the nearly uniform temperature resulting in heatpipes or two-phase systems.

A two-phase fluid loop evaporates the working fluid as it flows past payloads in a cold plate and condenses the working fluid in a heat sink. Since any heat added or removed from the fluid results in a phase change instead of a sensible heat change, nearly isothermal operation is realized in the loop. Furthermore, a properly designed two-phase loop will possess heat transfer coefficients in the evaporator and condenser sections which are orders-of-magnitude larger than those which exist in in pumped liquid loops. Thus, smaller temperature drops are experienced between the heat source/sink and working fluid. The small fluid mass flowrates required in two-phase loops require a small expenditure of electrical power if mechanical pumping is used. A two-phase system may also be capillary-pumped at no expenditure of electrical power.

1.1-3 Advantages of Heatpipe Radiators

Several deployable radiator concepts exist, including heatpipe radiators, moving belt radiators [2], liquid droplet radiators [3], and inflatable bag radiators [4]. Although the flight-proven heatpipe radiators possess a lower heat rejection capability per unit weight than the other concepts, they represent proven technology. They are free of the contamination, cost, mechanical, and survivability problems which plague these other designs. Unlike the other advanced radiator concepts, the heatpipe radiator does not impose stringent constraints on spacecraft slewing during radiator operation. Redundancy can be readily incorporated into a heatpipe radiator by including additional heatpipes to make up for those which might be lost during the mission due to micrometeoroid damage. Gas-loaded variable conductance heatpipes provide a variable thermal conductance between the heat dissipating payloads and the heat sink of space - thereby reducing spacecraft heater power requirements during cold case operation.

1.2 Theory of Operation

The thermal control system which will be tested in this experiment consists primarily of: (a) a capillary pumped loop (CPL), (b) the High Efficiency Thermal Interface (HETI), and (c) a heatpipe radiator. The fluid flow in this system is driven by capillary forces. Operation of the CPL and HETI are described herein.

1.2-1 Theory of Capillary Pumped Loop Operation

A basic CPL thermal bus consists of the following five pieces of hardware:

(1) one or more cold plates which consist of several wicked evaporators affixed to a mounting surface onto which heat dissipating payloads are attached, (2) a condenser or heat exchanger which transfers heat from the working fluid in the CPL to a heat rejection system (radiator), (3) a vapor transport line through which vapor generated in the cold plate is transferred to the condenser, (4) a liquid transport line through which liquid leaving the condenser is returned to the cold plate, and (5) an accumulator, which is a fluid reservoir used to control the loop liquid inventory and system saturation temperature. A simplified schematic of a CPL is shown in Figure 1-4. Detailed discussions of CPL operational principles and ground testing results appear in [5] and [6].

As is the case with a heatpipe, the driving force for fluid motion in a CPL is the pressure rise developed across the liquid-vapor interface in the wicked evaporator (see Figure 1-5). Addition of heat at this interface causes meniscus recession in the wick and produces a higher pressure on the vapor side of the interface than on the liquid side as a consequence of Laplace's Law ($\Delta p_c = 2\Sigma/r_p$, where Δp_c is the capillary pressure rise, Σ is the surface tension, and r_p is the effective pore radius of the wick material). This pressure rise is sufficent to force flow of vapor into the condenser and force flow of liquid back into the evaporator. When the evporator heat load, $\dot{Q}$, and fluid mass flowate, $\dot{m}$, (which are related by $\dot{m} = \dot{Q}/h_{fg}$, where h_{fg} is the fluid latent heat of vaporization) are sufficiently large, the total frictional pressure drop experienced throughout the loop, Δp_f, will exceed the maximum pressure rise which the wick material can sustain ($\Delta p_c < \Delta p_f$) and the system will deprime.

The accumulator is a thermally-controlled reservoir which helps set the system saturation temperature by forcing liquid into or out of the remainder of the CPL. If the reservoir is heated, causing the saturation pressure in the reservoir to exceed the saturation pressure in the remainder of the CPL, fluid will be expelled from the reservoir. The accumulator outlet has a fibrous wick structure so that only liquid may enter or exit the reservoir. When the reservoir is heated and liquid is forced out of it, this liquid will partially flood the condenser. This flooding has the effect of reducing the thermal coupling between the CPL working fluid and the heat sink, and will increase the saturation temperature in the loop. Similarly, cooling of the reservoir will draw liquid in from the condenser, increasing thermal coupling to the heat sink, reducing the loop saturation temperature.

The accumulator plays a vital role in CPL system startup. The CPL cannot

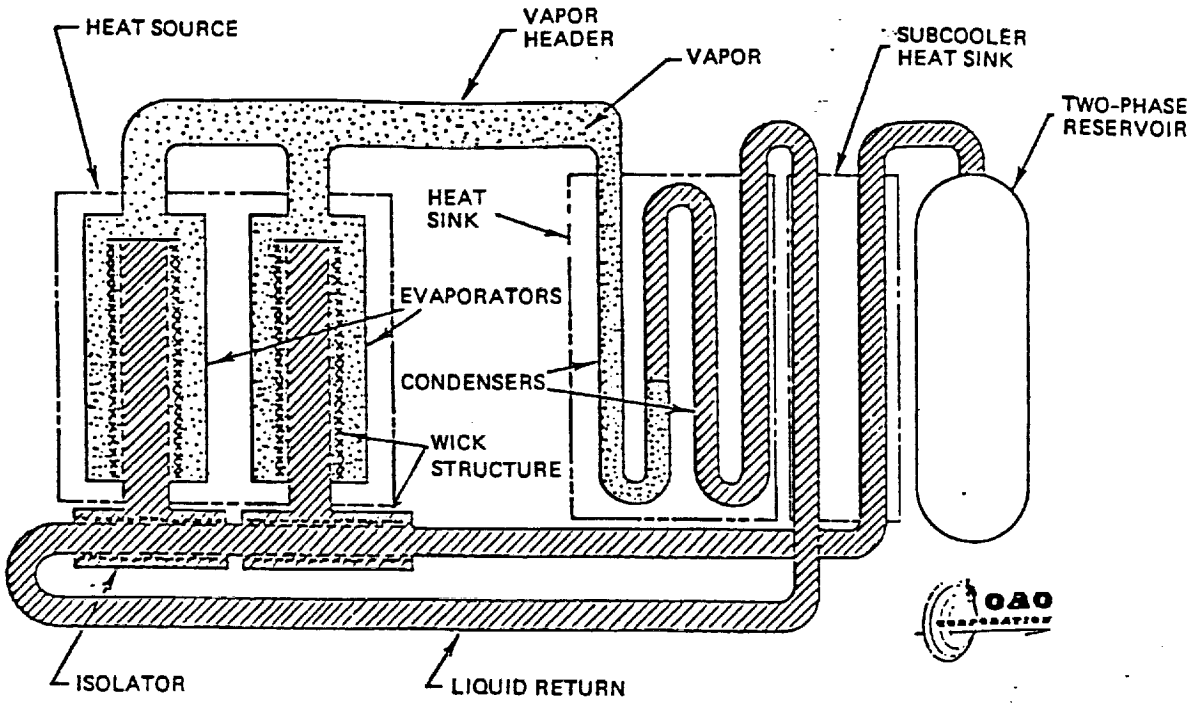

Figure 1-4. Schematic of a Capillary Pumped Loop (CPL)

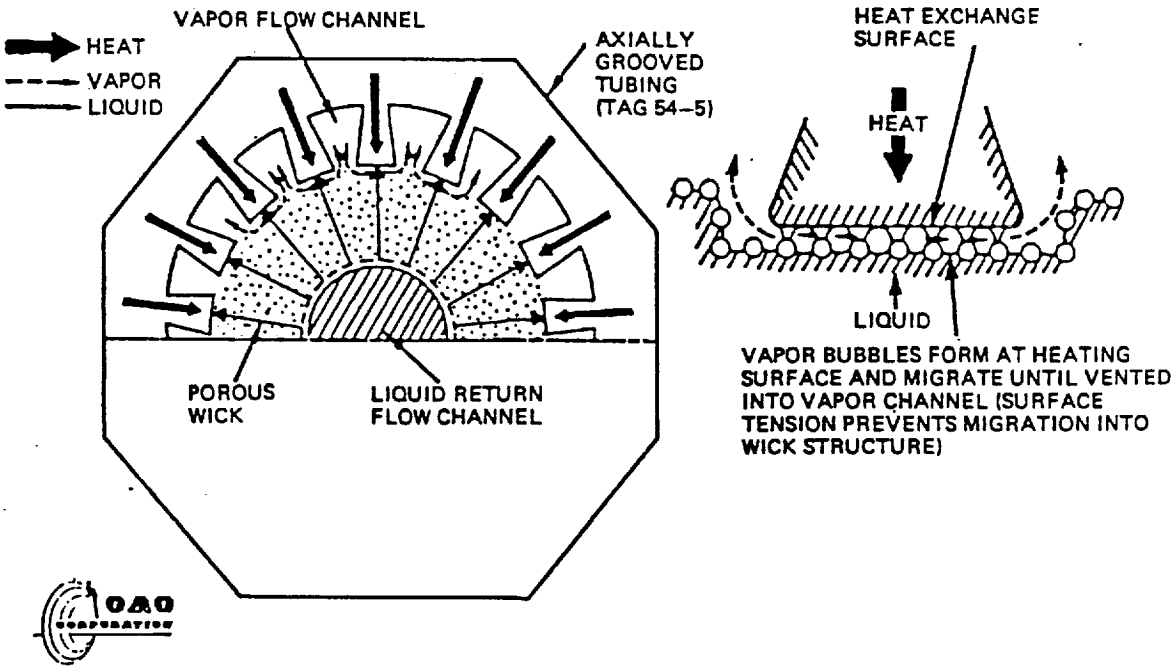

Figure 1-5. Cross-Section of the OAO Corporation CPL Evaporator Pump

sustain its design heat load unless the system is primed; i.e., the evaporator wick, evaporator liquid core, and liquid transport line are filled with liquid only. The safest (though perhaps not most weight-effective) way to prime the CPL prior to system startup is to flood the entire loop with liquid. This is accomplished by heating the reservoir above the loop temperature, thereby transferring liquid from the reservoir to the loop. Once heat is applied to the evaporators, the generated vapor forces the liquid which formerly resided in the vapor line and much of the condenser into the reservoir. Normal CPL operation then results.

The condenser section for prior ground and flight test CPL systems has consisted of single or multiple parallel serpentine tubes attached to a cooled plate. The generated vapor condenses on the tube wall and the condensate is dragged along the tube by vapor shear forces. A location is reached along the condenser where all of the vapor has been condensed; at locations downstream from this point, subcooling of the liquid takes place. Realistic condenser geometries for spacecraft applications have not been tested with CPL systems to this point.

1.2-2 Theory of High Efficiency Thermal Interface Operation

Like a heatpipe and a CPL, capillary forces drive fluid motion in the HETI. Figure 1-6 shows two views of the interior of the HETI which is used to transfer heat from a two-phase fluid loop to a heatpipe radiator. A manifold distributes vapor generated by the two-phase fluid loop to the evaporator ends of the radiator heatpipes. The vapor condenses on the grooved outer walls of these heatpipes. The latent heat released is conducted through the walls of the heatpipes to the inner surfaces where it vaporizes the heatpipe working fluid. These heat transport processes are inherently efficient (produce low temperature drops) and can be optimized by analysis to produce grooved surfaces with very high heat transfer coefficients.

An important consideration in the design is proper liquid management in a microgravity environment. As shown, a fibrous wick and a condensate collector tube are included at one circumferential point of the heatpipe. The fibrous wick transfers liquid from the condenser grooves on the heatpipe to the condensate collector tube which is at lower pressure due to capillary suction downstream at the evaporator. Residual condensation on the vapor manifold shell can be collected by either a fine mesh screen or circumferential grooves and transferred to capillary-sized holes on the condensate collector tube.

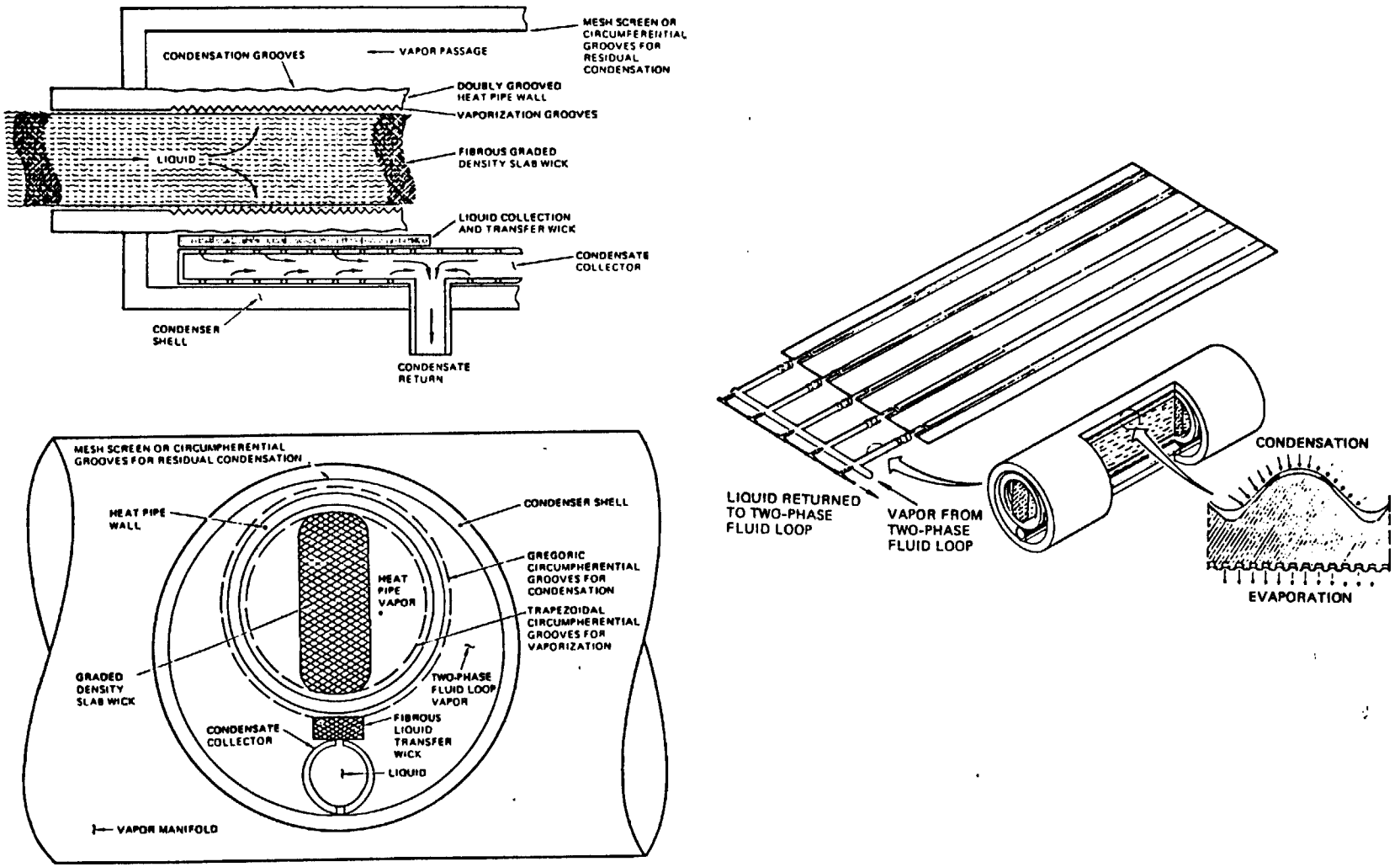

Figure 1-6. TRW-Developed High Efficiency Thermal Interface

1.2-3 Fluid Flow and Heat Transfer on Gregorig Grooves

The purpose for grooving the outer walls of the evaporator section of the radiator heatpipes is to produce large condensation heat transfer coefficients and minimize the temperature drop between the two-phase fluid loop vapor and the heatpipe. Geometries which promote very thin condensate films produce very high values of heat transfer coefficient (which equals, approximately, the ratio of liquid thermal conductivity to film thickness). Gregorig [7] performed the pioneering work on grooved condenser surfaces.

In order to understand the operation of these grooves, consider a thin condensate layer that flows from the groove tip to the valley. The condensate mass flowrate increase uniformly due to mass addition from a value of zero at the groove tip. The pressure drop in the liquid can be calculated as a laminar Poiseuille flow with a shear-free interface. It is possible to determine a groove profile which produces a constant condensate layer thickness and constant specified heat transfer coefficient.

The pressure in the liquid differs from that in the vapor due to capillary pressure generated by curved liquid-vapor interfaces. The profile of the groove is mathematically generated from the groove tip to the valley. At each point, the radius of curvature of the groove is selected so that the pressure induced in the liquid by capillarity exactly matches the pressure at that point resulting from viscous flow. Thus, at the groove tip, the liquid pressure is highest due to the convex curvature of the interface. As one progresses toward the valley, the magnitude of the radius of curvature increases as the pressure drops. As the inflection point of the groove profile is passed, the liquid-vapor interface becomes concave as the pressure continues to fall. The lowest liquid pressure occurs in the groove valley where the concave radius of curvature is the smallest.

1.2-4 Influence of Non-Condensible Gas on System Operation

An important consideration in this design is the effect of non-condensible gas on performance of the CPL and HETI. Small amounts of non-condensible gas will inevitably form in the two-phase loop as a consequence of chemical reactions between the working fluid and wall material. This gas is normally swept along by the vapor flow and collects at the coldest portion of the system. In conventional CPL condenser designs which consists of serpentine passages of tubing, the fluid leaving the condenser can consist of subcooled liquid with gas molecules which may either be dissolved in the liquid or may

exist as small bubbles in the liquid (depending on soluability of the gas in the liquid). If the latter case results, the gas can lead to CPL deprime and present great difficulties in recovering operation after deprime. In heatpipes, this gas is normally swept to the condenser end of the pipe where it forms a plug which effectively shuts off a part of the condenser.

The design of the HETI renders a CPL which includes it less susceptible to deprime caused by non-condensible gas. Any gas evolved over the life of the system should collect at the end of the HETI vapor chamber nearest the condenser section of the radiator heatpipes, instead of returning to the CPL evaporator through the liquid transport line. As is the case with heatpipes, uncontrolled generation of gas due to corrosion reactions can lead to complete blockage of the condenser section and failure of the thermal control system. This, however, is an unrealistic scenario in view of the elaborate processing steps taken with these systems to ensure that compatible materials are selected and gas-generating contaminants are excluded. In any event, the condenser section must be capable of collecting a small amount of gas without serious impact on condenser performance.

1.3 The Need for a Microgravity Flight Experiment

The flow of liquid in this system is strongly dependent on whether a gravitational field is present. This is especially true in the HETI, where the capillary forces which determine liquid flow patterns on the Gregorig grooves in microgravity are dominated by gravity forces during ground testing. Gravitational forces can greatly aid or hinder flow of liquid from the grooved exterior of the radiator heatpipes to the liquid collection tube. It will also have a major impact on heat transfer coefficients on both the exterior and interior surfaces of these heatpipes.

A commonly used quantity used to assess ground-testability of heatpipes is the static wicking height, which is the distance parallel to the gravity vector to which a liquid will "climb up" a specified wick structure. The static wicking height, H, depends on the effective pore diameter of the wick, D_p, surface tension, Σ, liquid density, ρ_l, and gravitational acceleration, g, as

$$H = 4\Sigma/(\rho_l g D_p)$$

In heatpipe testing practice, H sets a limit on the maximum diameter of slab wick heatpipes or a limit on adverse tilt for a wide variety of heatpipes if these pipes are to be ground testable. Consider liquid flow on grooves on the exterior of the radiator heatpipes for the case where the liquid collection

tube is on the "bottom" or "top" of the heatpipe. When the tube is on the bottom, liquid will drain condensate from the grooves and aid in filling of the tube. When the tube is on the top, the configuration is ground testable only if the static wicking height of the wick structure is at least as large as the outer diameter of the radiator heatpipe. The effective pumping pore diameter of the HETI is of the same magnitude as the Gregorig groove spacing. Typically, the Gregorig groove spacing is approximately 0.25 cm (see [8]), so if ammonia at 27°C is used as the working fluid ($\Sigma/\rho_l g = 3.39 \times 10^{-6}$ m^2), the upper limit on heatpipe diameter which will permit useful ground testing is 0.54 cm. Since this diameter is unrealistically small, it can safely be concluded that **the HETI cannot be tested on the ground without the location of the liquid collection tube having a major effect on liquid flow.** Gravity will not have such a pronounced effect on the behavior of the CPL and radiator fibrous slab wick heatpipes. The pumping pore diameters for the a CPL and a slab wick heatpipe are approximately 0.002 and 0.030 cm, respectively, so much higher static wicking heights are realizable with these components than with the HETI.

1.4 Prior Development Activities

The HETI was developed by TRW during the High Power Spacecraft Thermal Management (HPSTM) program sponsored by WRDC (contract number F33615-84-C-2414). The goals of this program were to: (1) develop a mathematical model of liquid flow on Gregorig-grooved surfaces, (2) verify experimentally the heat transfer coefficients predicted by theory, and (3) fabricate a 1-kilowatt HETI/radiator module.

1.4-1 Design of the High Efficiency Thermal Interface

The mathematical model of fluid flow and heat transfer on a Gregorig-grooved surface is presented in [8]. Four optimized groove profiles are shown in Figure 1-7. The profiles may be divided into crest and trough regions, with the separation point between the two regions located at the profile inflection point. The crest region is covered with a thin film of condensate (of the order of 0.001 mm) which possesses very high heat transfer coefficients (approximately 50,000 W/m^2-K). This represents heat transfer coefficients which are an order-of-magnitude larger than those observed in the evaporator and condenser sections of heatpipes. The more steeply shaped trough region (which has a circular profile) is filled with liquid and has significantly lower heat transfer coefficients than the crest region. The troughs serve as

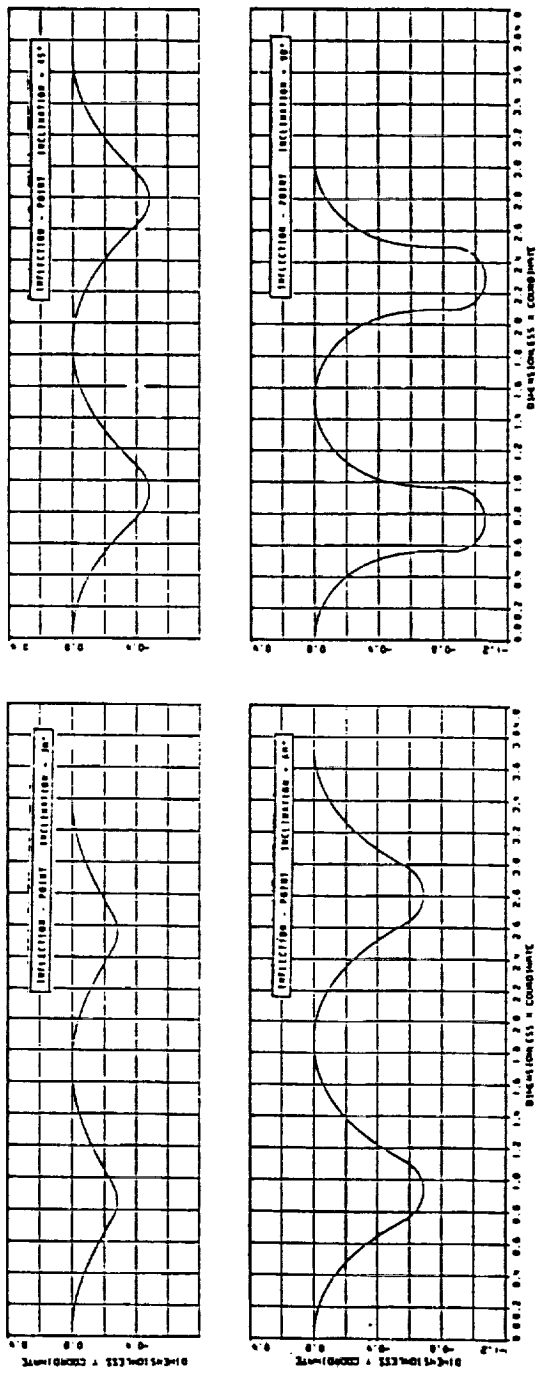

Figure 1-7. Practical Groove Profiles Constructed from Solution Curves with Circular Trough Tangent to Profiled Crest at Inflection Point

collection points for the condensate forming on the crests and are also channels for circumferential liquid flow into the fibrous wick and collection tube.

1.4-2 Experimental Verification of Mathematical Condensation Model

An experiment was performed to verify the very high heat transfer coefficients on Gregorig-grooved surfaces predicted by theory (see Figure 1-8). In order to minimize the effect of gravity, Gregorig grooves were cut onto a flat block of aluminum instead of being machined onto the exterior of a heatpipe. The selected groove dimensions (3.15 grooves per cm, inflection point at 45^{o}) were chosen so that that drainage of condensate from the crest to the trough was dominated by capillary forces instead of gravity forces. The grooved aluminum block was soldered onto a heatpipe and all other surfaces of the heatpipe protruding into the vapor chamber were insulated. A boiler supplied ammonia vapor to the condensing chamber and the vapor condensed on the grooved surfaces of the aluminum block. Condensate was drawn from the grooves troughs into a felt metal wick. The collected liquid fell from the wick in droplets intermittently due to gravity. The heat flow through the grooved surface was measured by a heat flux meter at the condenser end of the heatpipe. Thermocouples measured the temperature difference between the grooved block and the ammonia vapor. From this data, heat transfer coefficients on the grooved surface were measured.

The test was performed with the grooves pointing upward and with the grooves pointing downward. It was surmised that, when the grooves are pointing upward, gravity aids drainage of condensate and the resulting heat transfer coefficients would be slightly larger than would result in zero-g; when the grooves are pointing downward, gravity hinders drainage of condensate and slightly lower heat transfer coefficients would result. However, the opposite trend was noted, with the heat transfer coefficients for upward- and downward-facing grooves being 33.5 kW/m^2-K and 69.2 kW/m^2-K, respectively. The expected value for both orientations was 47.0 kW/m^2-K. This discepancy is believed to be due a faulty method for draining the groove troughs. When the grooves faced upward, a thick liquid film could build up until the moment when a liquid ammonia droplet would fall from the hanging felt metal wick. The liquid in the troughs would then flow into the wick, producing a thin film until condensation thickened the film, with low average heat transfer coefficients resulting. When the grooves faced downward, liquid probably dripped off the grooved suface

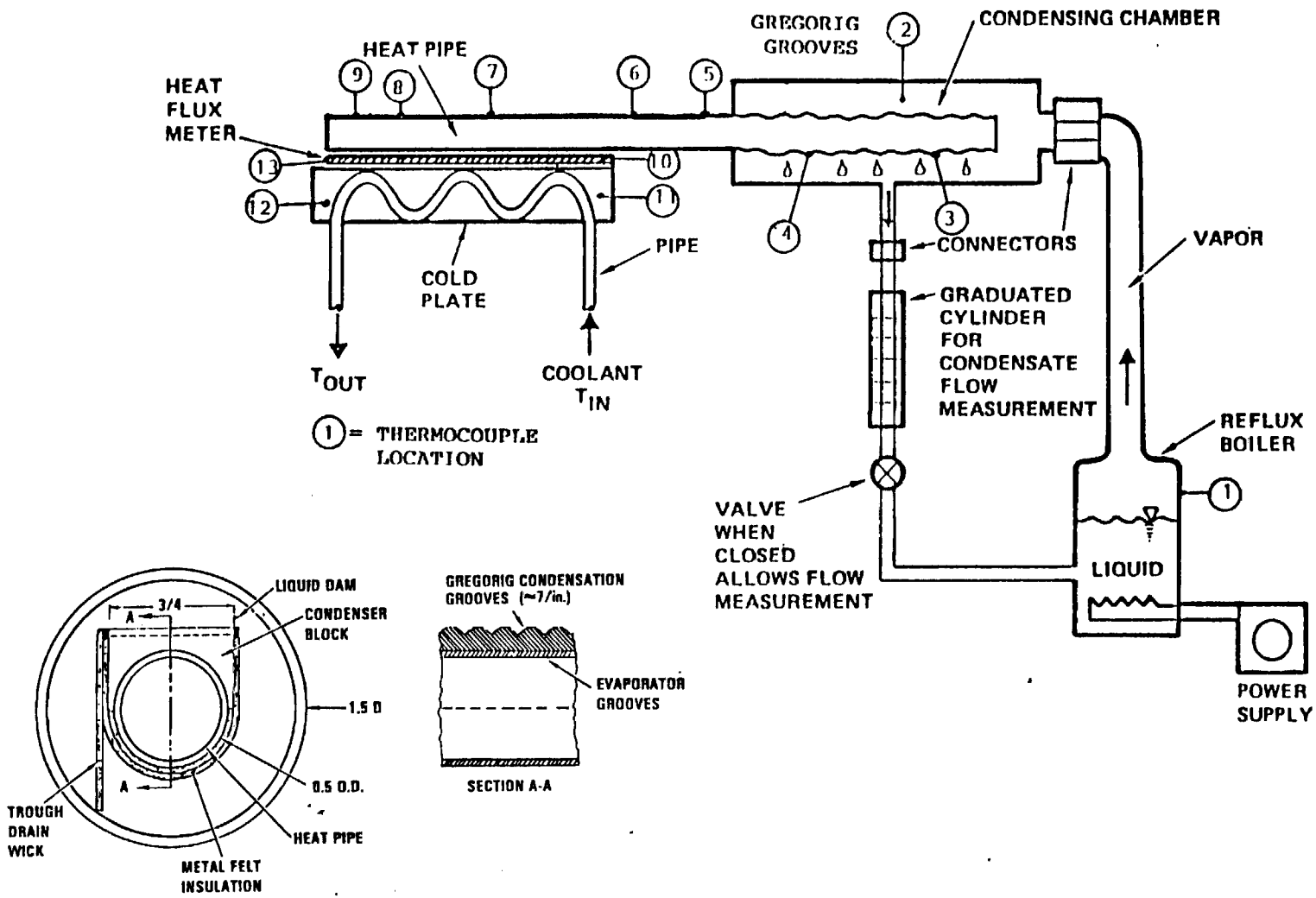

Figure 1-8. Diagram of Test Apparatus Used in HPSTM Study to Measure Heat Transfer Coefficients on Gregorig-Grooved Surfaces

at the dam, producing artificially high heat transfer coefficients. The test could not be repeated after correcting this drainage problem due to program schedule and cost constraints.

1.4-3 Fabrication of the HETI/Radiator Module

Piece parts for a five-heatpipe HETI were fabricated under the High Power Spacecraft Thermal Management contract. The components constructed include heatpipes, a vapor chamber, liquid collection tubes, and liquid collection fibrous wicks. The heatpipes were constructed of aluminum, while the remaining parts were stainless steel. The Gregorig grooves on the exterior of the evaporator sections of the five heatpipes were machined using a numerically-controlled lathe. The heatpipes were affixed to the HETI vapor chamber by Swagelok fittings. Cost constraints prohibited final assembly. The mechanical design and fabrication effort established that a radiator module with a Gregorig groove high-efficiency interface is practical and can be easily fabricated with advanced numerically-controlled machining.

2. EXPERIMENT OBJECTIVES

There are several objectives of this experiment, ranging from basic science issues such as determination of heat transfer coefficients to practical engineering concerns such as understanding of the flow dynamics of the entire thermal control system. These objectives are described in greater detail below.

2.1 Measurement of Heat Transfer Coefficients

The desire to minimize temperature drops in the thermal control system between the payload and radiator mandates designs which maximize heat transfer coefficients to the greatest extent practical. In this experiment, we will be concerned primarily with determination of heat transfer coefficients on the Gregorig-grooved surface of the HETI, as well as the evaporator and condenser sections of the radiator heatpipes.

2.1-1 Heat Transfer Coefficients in the HETI

The HETI and radiator heatpipes in this experiment will be instrumented with thermistors in a manner which will permit calculation of the average heat transfer coefficient over the Gregorig-grooved surfaces on the exterior of the radiator heatpipes. Calculation of this quantity requires measurement of the CPL vapor temperature, heatpipe evaporator wall temperature(s), and CPL evaporator heat load. Heat transfer coefficients will be measured at various working fluid temperatures and heat loads and compared to the theory described in [8].

2.1-2 Heat Transfer Coefficients in Heatpipes

Calculation of heat transfer coefficients in the evaporator and condenser sections of the fibrous slab wick radiator heatpipes can be made from knowledge of evaporator tube wall temperatures, condenser tube wall temperatures, adiabatic section wall temperature (which is extremely close to the heatpipe vapor temperature), and CPL evaporator heat load. These measurements will also be performed at various working fluid temperatures and heat loads. These results will be compared with ground test data and available mathematical models of evaporation and condensation in circumferentially grooved tubing. For comparison purposes, the measured heat transfer coefficients for these heatpipes in ground tests are typically one to two orders of magnitude smaller than those expected for the Gregorig grooves in zero-g.

2.2 Integrated CPL/HETI Operation

The behavior of conventional CPL systems which condense vapor in a

serpentine length of smooth tubing is fairly well understood. Small temperature and pressure oscillations, which would have been nearly impossible to predict analytically, were observed in both ground and flight tests (see [6] and [10]). These oscillations, however, did not seriously degrade CPL performance. Two-phase flows of liquid and vapor are not amenable to the type of linearized stability analysis which can determine whether small oscillations will be undamped and grow to the point where they can cause unacceptable temperature oscillations in the payload or produce CPL deprime. Therefore, flight testing of new two-phase flow systems remain the only method to ascertain with any certainty whether such systems will exhibit stable behavior.

2.2-1 System Startup Transients

During the early development of CPL systems with condenser tubing, the priming and startup procedures posed some difficulties. After pressure priming flooded the system with liquid and the CPL evaporator pumps were heated, the cold liquid which initially resided in the condenser was forced into the reservoir. This tended to drop the system saturation temperature and deprime the CPL since the liquid in and near the evaporators became superheated. This problem was later circumvented by raising the condenser sink temperature prior to startup.

Use of the HETI instead of condenser tubing will alter the CPL startup behavior due to the different thermal conductance between the liquid which floods the HETI prior to startup and the heat sink. The startup process can be characterized reliably only by experimental means. One objective of this experiment is to determine reliable startup strategies which do not result in evaporator deprime.

2.2-2 Vapor Flow Distribution in the HETI

It is desired to have equal mass flowrates of vapor enter each manifold of the HETI to better effect isothermal radiator operation. Asymmetry in vapor flow will result in different heat throughputs for each vapor chamber/heatpipe combination and a radiator with nonuniform temperature zones. In order to verify equal flow distribution among the two vapor chambers, the thermistors on each radiator heatpipe will be monitored to detemine whether heat throughputs for these pipes are equal.

2.2-3 Effect of Non-Condensible Gas on System Operation

During the final stage of the flight test, a non-condensible gas contained in a reservoir will be slowly leaked into the CPL vapor line. The goal of this

portion of the test is to determine whether this gas will induce CPL deprime, or whether it will collect at the downstream end of the HETI and form a gas plug in the same manner as would result in a gas-loaded heatpipe. The result of this final phase of the experiment will be an assessment of whether the CPL/HETI combination is more gas-tolerant than earlier CPLs with a shear-driven, flow-through condensers.

2.3 CPL Accumulator Dynamics

The accumulator is one of the most important - yet probably the least understood - component of a CPL system. The relationship between the accumulator-to-condenser temperature difference and the accumulator fluid intake/expulsion rate is not known. If the condenser geometry and intake/expulsion rate are known, their effect on condenser blockage and CPL saturation temperature can be determined. Knowledge of this relationship is essential to mathematical modeling of transient CPL behavior and design of new CPL systems.

During all operational phases of the experiment, the liquid mass flowrate entering or leaving the accumulator will be monitored using a suitable flowmeter. The purpose of this measurement is to determine a relationship between accumulator fluid intake/expulsion rates and temperature differences between the reservoir and CPL vapor. This data will assist in development of mathematical models for CPL behavior.

3. EXPERIMENT PAYOFFS AND BENEFITS

The goals of this NASA IN-STEP program are consistent with the objectives of NASA/OAST as enumerated in Reference [9]. This program offers the government benefits from the viewpoint of: (1) providing data which will aid in understanding liquid-vapor flows in microgravity; and (2) assessing the thermal performance of a versatile, highly efficient, spacecraft thermal control system which is applicable to high power missions for NASA and other government agencies.

3.1 Fundamental Information on Microgravity Fluid Behavior

Two-phase flows of liquid and vapor cannot often be modeled accurately using analytical techniques only. The relative orientation of the liquid and vapor phases has a major impact on the fluid flow and heat transfer processes. Experimental data, which are required to verify predictions of analytical models, are often the only design tools available to the thermal control engineer when flow patterns are very complex. Two payoffs of this experminent are: (1) measured heat transfer coefficients on the Gregorig-grooved surface of the HETI and in the evaporator and condenser sections of circumferentially-grooved slab wick heatpipes; and (2) thermo-hydraulic data for a wicked CPL accumulator which will aid in understanding of the accumulator operation and permit development of CPL math models with higher degrees of versatility and fidelity than currently exist.

3.1-1 Heat Transfer Coefficients

Minimization of TCS temperature drops and maximization of heat transfer coefficients results in weight and area savings for high power spacecraft which require deployed radiators. In radiator heatpipes which possess long condenser sections, relatively low heat transfer coefficients do not produce appreciable temperature drops between the heatpipe fluid and the tube wall because of the large area over which condensation is taking place. In applications where short condenser sections are mandated by configurational constraints (e.g., cascaded heatpipes, which are arranged in series with the condenser section of an "upstream" pipe coupled to the evaporator section of a "downstream" pipe), low heat transfer coefficients can result in large temperature drops since the condensation area is small.

Mathematical modeling of fibrous slab wick heatpipes requires knowledge of the heat transfer coefficients in the evaporator and condenser sections of the heatpipe. No reliable analytical models exist for prediction of heat transfer

coefficients for this geometry. Ground test data is often used in the absence of other data. However, gravity will probably promote drainage of liquid from the tube wall. This will result in higher measured heat transfer coefficients in one-g conditions than will probably exist in microgravity.

The heat transfer coefficient measurements which will be made during this experiment in the HETI and heatpipes will provide fundamental data which can verify or disprove models of film flow with heat addition or removal, and produce evidence which will prove or refute the notion that heat transfer coefficients for slab wick heatpipes measured in one-g conditions can be applied to microgravity conditions.

3.1-2 Thermohydraulics of a Wicked CPL Reservoir

A CPL reservoir is faced with many of the same liquid acquisition or collection concerns as propellant tanks in microgravity. In the case of a CPL reservoir, liquid acquisition is achieved using screens or fibrous wick structures which line the reservoir walls and extend into the center of the reservoir.

A major shortcoming of CPL analysis codes is the fact that they cannot automatically determine the loop saturation temperature as a function of time in the simulation. This important quantity must be provided by the user, even though it is set physically by the CPL heat throughput and its coupling to its environment. Although it is possible to determine an effective thermal conductance between the CPL working fluid vapor and the heat source or sink, this task is considerably more difficult for a reservoir. The conductance between the reservoir vapor and the reservoir wall depends strongly upon the reservoir wick structure and the internal orientation of the liquid and vapor phases. This conductance will also have a bearing on the relationship between reservoir heat input (producing a saturation temperature and pressure rise) and liquid expulsion rate. The instrumentation included on the CPL reservoir and its outlet line in this experiment will provide valuable data for validating analytical models of reservoir behavior. The benefits of this task have potential spillovers into the area of propellant acquisition using wick structures.

3.2 Microgravity Behavior of an Integrated Two-Phase Thermal Control System

Flight experiments involving two-phase flows have consisted almost entirely of single components. Usually, tests or analyses of single components of two-phase systems cannot be used to determine with any certainty the thermo-

hydraulic behavior of an integrated TCS consisting of multiple components. For instance, it would be difficult to determine a priori whether the CPL/HETI system would be more susceptible to pressure and/or temperature oscillations than a CPL with shear-driven condensation in tubes. This IN-STEP experiment will verify the principles of operation for a small-scale, integrated heat transport/rejection system with all of the interfaces and components which would exist in a flight system.

3.3 Applications to Missions for NASA and Other Government Agencies

Figure 3-1 shows a deployable radiator system which would employs components of the TCS which will be tested in this experiment. The figure demonstrates modularity of the design. Radiator systems with various power dissipation requirements can be constructed utilizing the appropriate number of HETI/radiator segments.

The concept shown in Figure 3-1 is a survivable system. The radiator would be designed with a sufficient number of redundant heatpipes to make up for those expected to be damaged over the life of the mission due to spaceborne debris or micrometeoroids. The compact HETI may be shielded against penetration without a large weight penalty.

The combination of near-isothermality, modularity, survivability, no pumping power, and advanced state-of-development make this CPL/HETI/heatpipe radiator system well-suited for a wide range of NASA and DoD missions with heat loads of 5-10 kW or greater.

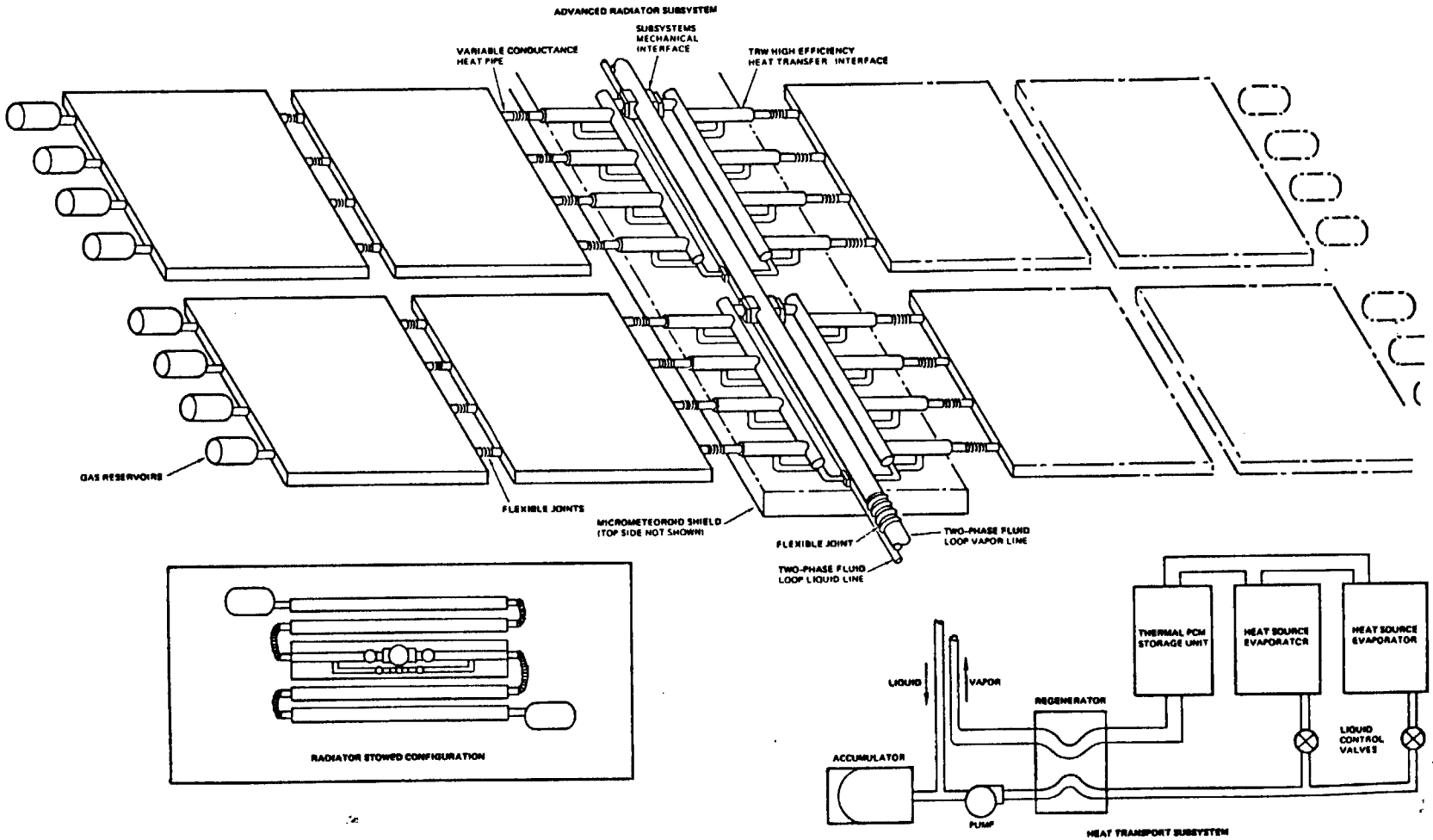

Figure 3-1. Sample Configuration of a Modular, Survivable, Deployable, Two-Phase Thermal Management System

4. EXPERIMENT DESCRIPTION

The section describes a preliminary design of the integrated CPL/HETI/heatpipe radiator flight experiment. The experiment is configured as a Hitchhiker-G (HH-G) payload using a Get-Away Special (GAS) canister. The rationale for the HH-G selection is discussed. The required instrumentation and control hardware are also described.

4.1 Selection of Experiment Carrier

The Hitchhiker-G (HH-G) carrier using a GAS-type canister was selected for this experiment because of its operational versatility and the prior success of a CPL flight experiment which used the HH-G. The Hitchhiker-M carrier was not selected because this experiment could be contained in a much smaller envelope than Hitchhiker-M payloads normally require. The Complex Autonomous Payload (CAP) carrier was not selected because the potential complications which might arise during startup could produce a low likelihood for mission success without experimenter interaction during this crucial phase of the testing program. Specific reasons for the HH-G selection are given below. This selection was guided by STS carrier descriptions appearing in References [11] and [12].

1) The ability to send real-time commands to the experiment greatly increases the versatility of the test. This feature is especially useful during system startup and recovery from CPL deprime.
2) The HH-G provides sufficient electrical power for heaters to stress the heat transport limits of the TCS, unlike the CAP carrier where electrical power must be provided by batteries and available power is limited.
3) The "transparent" data and command interface allows the experimenter to issue commands and receive data from the payload during flight using the same Customer-provided Ground Support Equipment used during the payload assembly and checkout process.

4.2 Experiment Components

The thermal control system (TCS) which is being tested consists of an HETI, CPL, and heatpipe radiator. These components are described in detail below. The entire TCS will use ammonia due to its desirable properties as a working fluid for CPLs and heatpipes. The TCS will be attached to the top plate of the GAS canister and configured so that ground testing may be performed with some measure of success (albeit, gravity-aided) to assess experiment integrity during preliminary checkout testing and subsequent thermal vacuum testing. The configuration of the TCS on its circular mounting plate is

shown in Figures 4-1 and 4-2. This mounting plate will serve as the radiator for heat added to the evaporator pumps of the CPL. This configuration is patterned after the CPL GAS and H/H-G flight experiment designs (see [10]).

4.2-1 High Efficiency Thermal Interface

The HETI included in this experiment will have two vapor chambers to accommodate the two radiator heatpipes. The location of the liquid collection tube in each chamber will be at the "bottom" of the radiator heatpipes; i.e., on the opposite side from the radiator plate. This orientation will permit gravity-aided drainage of the Gregorig-grooved surfaces during ground testing.

4.2-2 Capillary Pumped Loop

The CPL design which will used in the experiment is very similar to the CPLs which have flown on the previous GAS and H/H-G experiments. It will possess two evaporator pumps plumbed in parallel containing isolators to prevent a deprime which might occur in one pump from propagating to the other. The evaporator wick pore size will be approximately 10 micrometers. This small pore will produce a large enough static wicking height that the CPL can operate satisfactorily during ground tests, even though all CPL components do not lie in the same horizontal plane. CPL startup will be achieved using the reliable flooding procedure described above. The maximum total evaporator power will be 600 watts.

The accumulator will have a wicked internal construction for liquid acquisition and a wicked outlet to ensure that only liquid leaves the accumulator when it is heated. The accumulator will be provided with a heater for saturation temperature control and will possess some thermal coupling with the top plate of the canister, which acts as the heat sink. The line connecting the accumulator with remainder of the CPL will be well-coupled to the heat sink plate to provide some liquid subcooling. A flowmeter will be inserted in the accumulator outlet line in order to measure liquid intake or expulsion rates during testing. Correlation of these flowrates with temperature differences between the reservoir and CPL vapor will result in more physically sound thermal modeling techniques for CPL systems.

4.2-3 Heatpipe Radiator Plate

Two fixed conductance fibrous slab wick heatpipes will transfer heat from the HETI to the radiator plate. The exterior surface of the radiator plate will be covered with silvered teflon tape, whose solar absorptivity and IR emissivity are 0.10 and 0.78, respectively. These thermo-optical properties

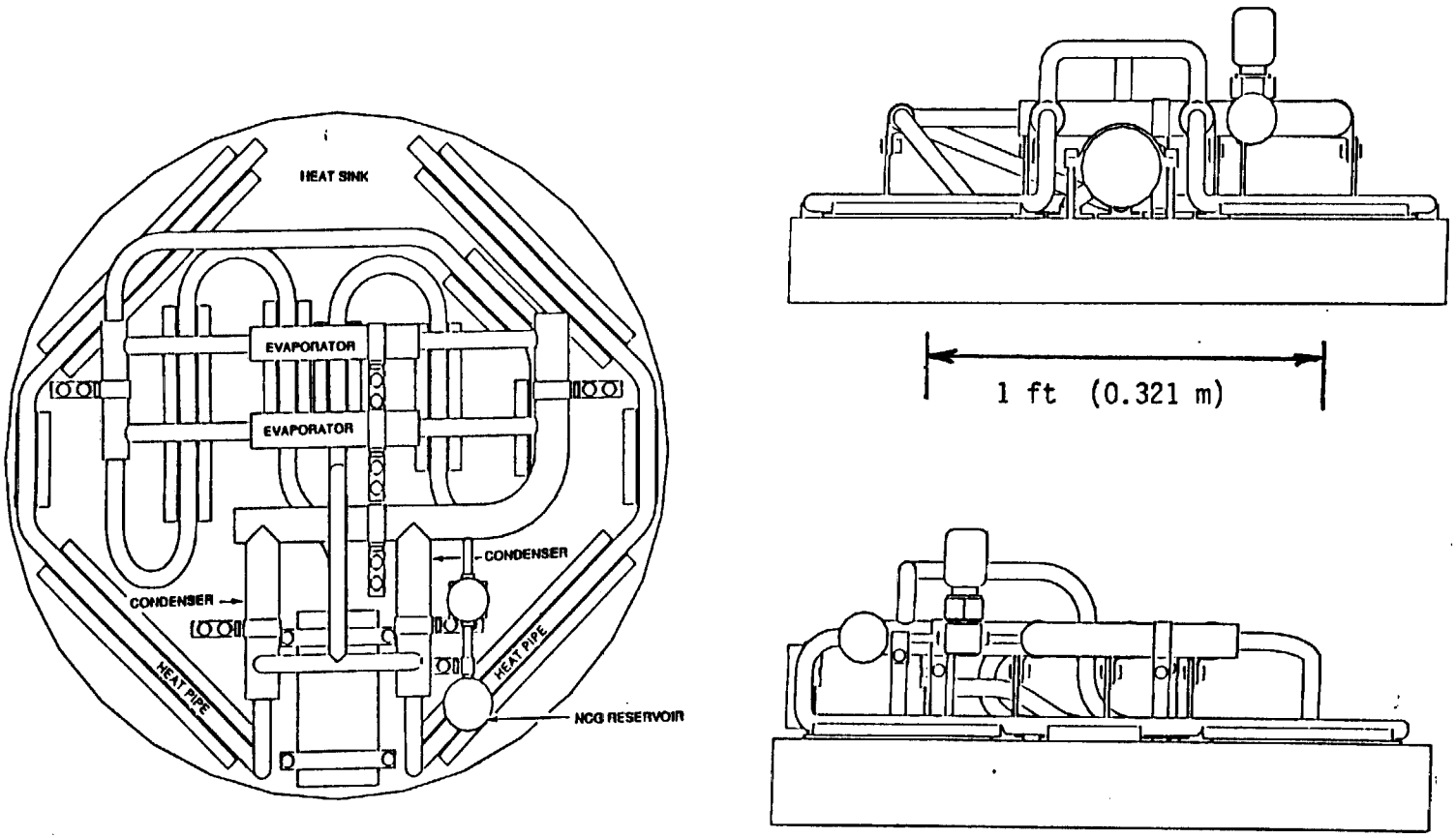

Figure 4-1. Preliminary Experiment Layout on Mounting Plate (Side and Top Views)

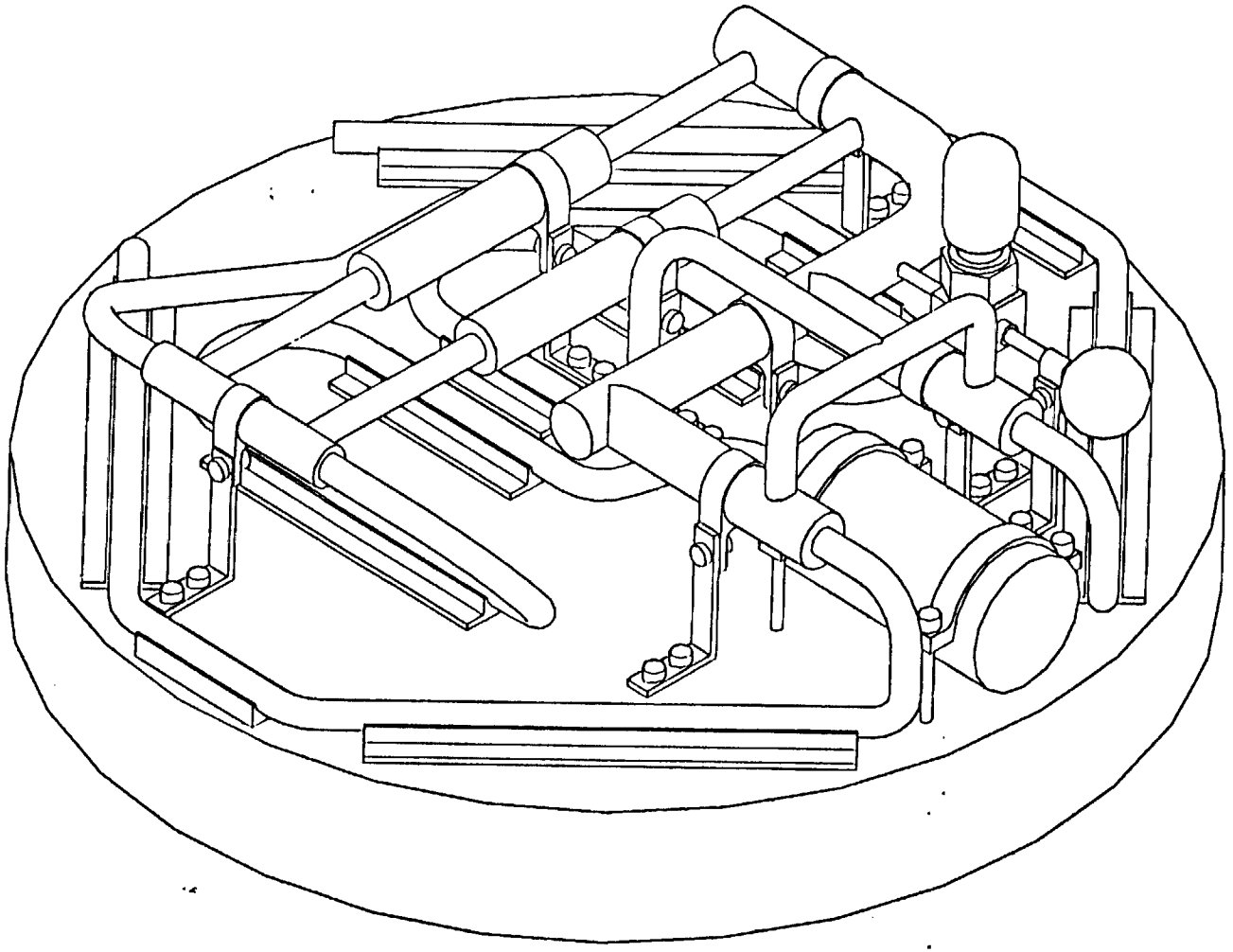

Figure 4-2. Preliminary Experiment Layout on Mounting Plate (Isometric View)

produce a radiator which can efficiently radiate heat produced in the CPL, while absorbing little sunlight which may impinge upon the radiator.

This experiment will be heat sink limited; i.e., there is insufficient available radiator area to dissipate the maximum heat load (600 watts) at steady state at the maximum system operating temperature (50°C). Thus, operation at the maximum heat load will be initiated once the canister has cooled to a low temperature (roughly 0°C) and can be sustained until the TCS temperature reaches its maximum temperature of 50°C. The top plate of the canister will be constructed from approximately 60 kg of aluminum or other suitable material with a large specific heat and thermal conductivity. If the plate is aluminum, continuous operation at 600 watts can be maintained for 30 minutes. Once the TCS reaches 50°C, testing activities should be suspended until its temperature cools to an acceptable level. The exact waiting period will depend on the Shuttle orientation with respect to the sun and earth, but will typically range from two to six hours.

The two fixed conductance radiator heatpipes used will be 1.27 cm OD graded-porosity fibrous slab wick pipes. Although the maximum heat load which can be carried by heatpipes with this wick structure and effective length is 450 watts, the maximum design heat load per pipe for this experiment is 300 watts. The condenser sections of the heatpipes will be attached to the radiator plate using aluminum saddles with a room-temperature vulcanized (RTV) silicone rubber interface filler. These heatpipes are bent to increase the length of contact between the pipes and radiator. During ground testing with the radiator plate topmost, the heatpipes will operate in reflux mode (with the condenser section above the evaporator section to provide gravity-aided liquid return to the heat source).

4.2-4 Heaters, Thermistors, and Data Acquisition Equipment

This experiment will be provided with space-qualified tape heaters for the CPL evaporator pumps, CPL reservoir, non-condensible gas reservoir (to prevent condensation of ammonia in the reservoir after the solenoid valve is actuated), data acquisition hardware, and command and control hardware. All heaters except for the CPL evaporator heaters will be thermostatically controlled with the required redundancy incorporated in the heater control design.

The experiment will be instrumented with YSI 44006 thermistors or acceptable equivalent. The thermistors will be calibrated such that 0 to 5 volts correspond to 270 to 340 K. The voltage outputs of the thermistors will

be sampled using an analog multiplexer and output to the analog data channel. This data channel provides a 10 Hz index pulse which will be used to advance the multiplexer. The data is quantized into 8 bits, yielding a temperature resolution of 0.27°C over the stated temperature range. It is anticipated that the experiment will require less than 50 analog instruments (including thermistors). Thus, the period required to sample the entire experiment will be less than five seconds. In addition to the analog channel, HH-G provides three channels which permit measurement of payload temperatures and pressure, even when the payload is off. Use of these additional channels to measure the temperatures at the expected warmest and coolest locations in the canister allows the analog channel to cover a smaller temperature range, thus increasing the resolution with which their thermistors will read. The analog channel is used for data acquisition instead of the available asynchronous channel because the design of flight electronics is much simpler for analog data. Although the asynchronous channel can provide higher resolution and a higher sampling rate, it is felt that use of the analog channel provides simplicity with acceptable performance.

The data from this experiment will be received by an HP 9000 series 300 computer with an RS-232 port. The Customer-provided Ground Support Equipment (CGSE) will be equipped to handle analog data during testing and asynchronous data from the Customer Carrier Ground Support Equipment (CCGSE) during flight operations. Additional hardware and software will be provided to give near real-time graphical data display and data storage on suitable media. Figure 4-3 shows a block diagram describing the flow of data.

4.2-5 Experiment Command and Control Equipment

The CGSE will use the asynchronous uplink to issue commands to a logic circuit in the experiment. The logic circuit interprets the command and sends a signal to a relay driver circuit which energizes the CPL evaporator heaters, gas reservoir solenoid valve, or cooling fan. Each evaporator will have five heaters which will allow for discrete power settings ranging from 25 to 300 watts per evaporator. Data on the relay position (open or closed) will be passed to the analog data acquisition system. Although asynchronous control requires some digital flight hardware, it provides near real-time control with great flexibility. In addition to the command control of the evaporator heaters, the heater control circuit will be equipped with a thermostat which will prevent evaporator temperatures from reaching 80°C in the event of a

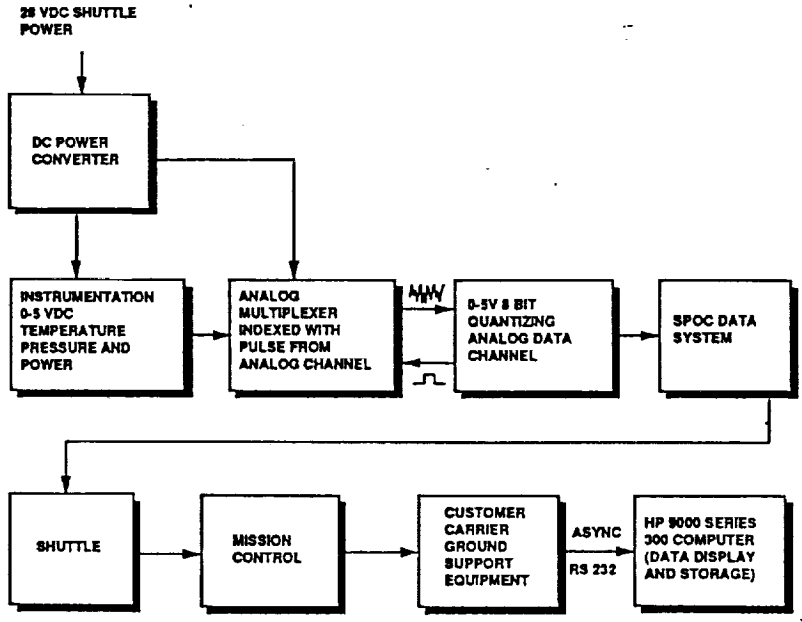

Figure 4-3. Data Acquisition System Operation

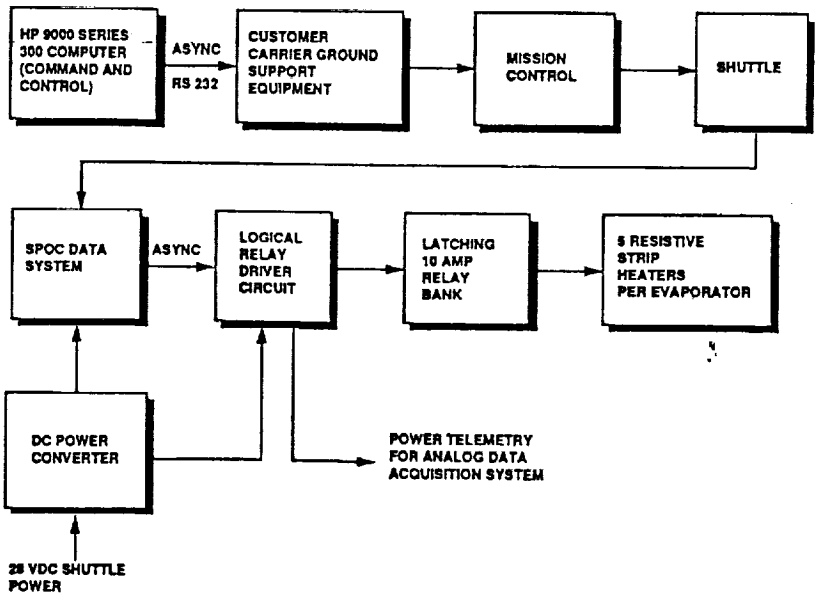

Figure 4-4. Command and Control System Operation

failure in the primary control system. Figure 4-4 shows a block diagram describing the command and control system operation.

4.2-6 Non-Condensible Gas Reservoir

A reservoir containing a non-condensible gas (probably helium) will be included in this experiment. The purpose of this reservoir is to gradually leak the gas into the CPL to determine its effect on CPL operation. In particular, it is desired to determine whether this gas causes a CPL deprime. It is expected that the injected gas will collect at the downstream end of the vapor chambers of the HETI and form a nearly impermeable barrier to vapor flow. The reduced thermal conductance between the CPL working fluid and the heat sink will cause the CPL evaporators to show an increase in operating temperature for a fixed heat load than it would experience at the same heat load with no gas present.

The pressurized gas will be leaked into the CPL upon actuation of a solenoid valve in the line between the gas reservoir and the CPL. This line will also contain a very small orifice to ensure that the gas is leaked into the CPL over a period of hours. Rapid expulsion of the gas into the CPL would probably result in CPL deprime and would cause an unrealistic assessment of the effect of gas on the system since non-condensible gas is evolved very slowly in a properly processed CPL. The exhaust port for the gas reservoir will be in the vapor line of the CPL. The injection of gas in the CPL will be the last phase of the microgravity testing performed on the TCS.

4.2-7 Auxiliary Hardware

The GAS canister will be pressurized with helium to a pressure of approximately 0.1 MPa (1 atm). This helium will aid with cooling of the support electronics equipment which cannot be mounted on radiator surfaces. A small fan of the type used in the CPL HH-G flight experiment will be used to circulate the helium in the canister during periods when the CPL evaporator pumps are not heated. The sides of the GAS canister will be left uninsulated so that additional canister area is available for heat rejection. This approach will reduce the duration of cooldown periods between phases of experiment operation at high power levels. Helium was selected as the gas instead of nitrogen because of its higher thermal conductivity and expected heat transfer coefficients.

5. EXPERIMENT DEVELOPMENT OUTLINE, SCHEDULE, AND COST

This chapter presents the experiment outline and anticipated schedule and costs for both Phases B and C/D. As might be expected, the cost and schedule for Phase B are known with greater certainty than the costs for Phase C/D. The goal of the Phase B development is an experiment design which has matured to a point approaching the Critical Design Review stage. Phase C/D includes final detailed design, fabrication of the flight experiment, integration with the HH-G, qualification testing, Orbiter integration, flight operations, and post-flight data analysis and reporting.

5.1 Phase B Activities

During Phase B, the following activities are planned: (1) an experiment to verify heat transfer coefficients on Gregorig-grooved surfaces predicted by the mathematical model in [8]; (2) mechanical design of the experiment; (3) detailed thermal design of the experiment; (4) structural analysis for pressure containment and launch loads; (5) design of data acquisition and control hardware and software; (6) test of a breadboard model of the TCS; and (7) preparation of the necessary safety and manifesting documentation. Testing of all critical components will be completed during Phase B.

5.1-1 One-G Gregorig Groove Condensation Heat Transfer Coefficients

The experiment described in Section 1.4-2 performed under the HPSTM Study measured unrealistic values of condensation heat transfer coefficient on horizontal Gregorig-grooved surfaces. This was caused by a flaw in the experiment setup which did not properly use the felt metal wick to remove liquid from the groove troughs. As a consequence of this, the test was unable to accurately ascertain the thermal performance benefits offered by Gregorig grooves.

In order to properly measure the heat transfer enhancement offered by these grooves, a new thermal test will be performed very early in Phase B of this IN-STEP program. Instead of using the apparatus shown in Figure 1-8 from the previous test, the planned experiment will attach the fibrous wick used to drain the Gregorig groove troughs directly to the vapor chamber wall, which is heated locally (see Figure 5-1). The aluminum block containing the Gregorig grooves is soldered to a heatpipe. This end of the heatpipe is encased in a chamber which is partially charged with ammonia. All surfaces of the heatpipe in the chamber and the aluminum block (except for the grooved surface) are covered with a felt metal wick which serves as an insulator. The other end of

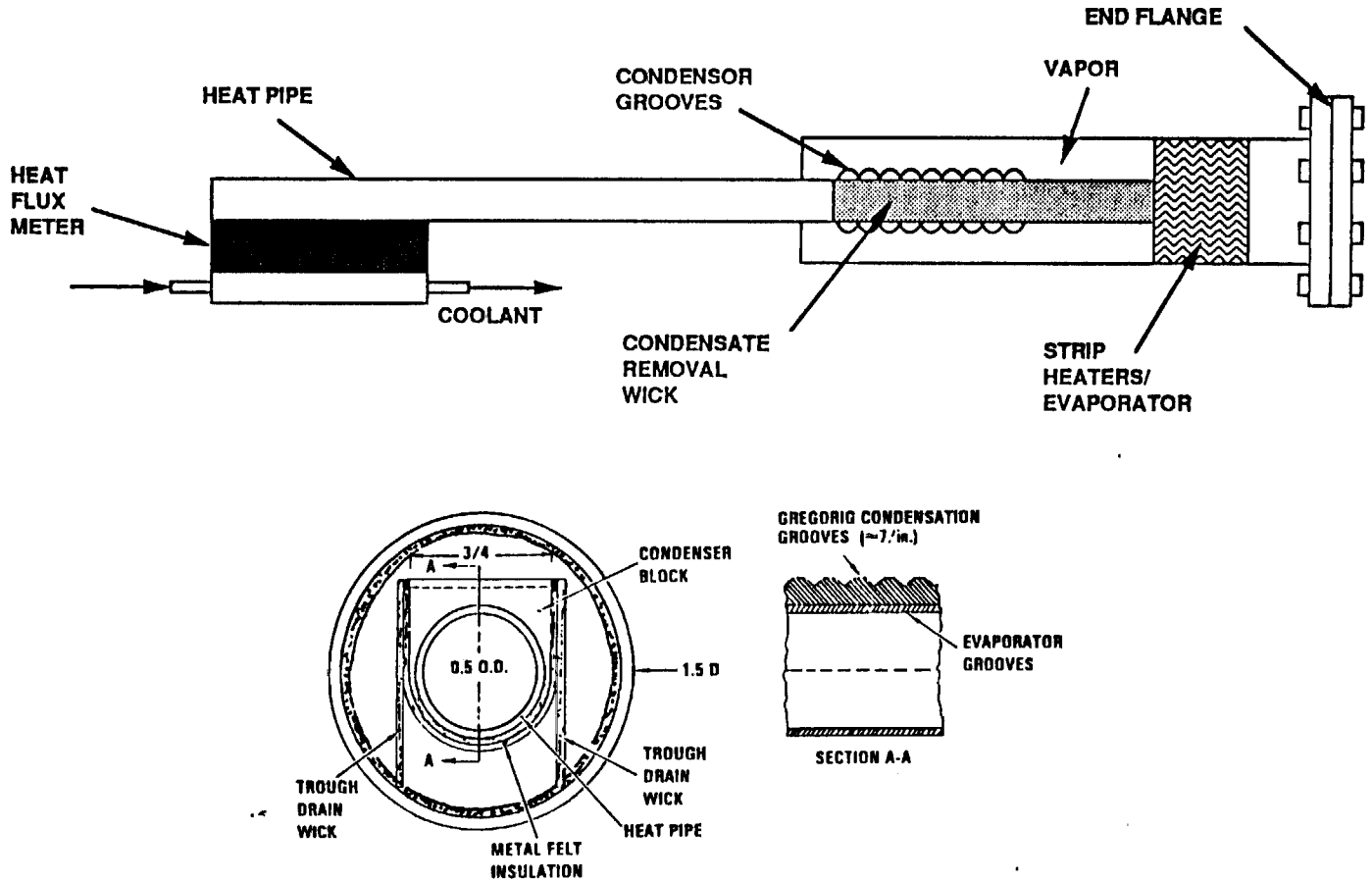

Figure 5-1. Diagram of Test Apparatus to be Used in IN-STEP Phase B Program to Measure Heat Transfer Coefficients on Gregorig-Grooved Surfaces

the heatpipe is soldered to a saddle. Attached to this saddle are a stainless steel block of known thickness and a copper block containing a cooling coil through which liquid nitrogen is circulated. Thermocouples are attached to the two sides of the stainless steel block, so that by measuring these temperatures, one is able to determine the heat flow through the stainless steel block (which equals the heat flow through the heatpipe and heat released by condensation on the grooved aluminum block at steady-state conditions). Thermocouples also measure the temperatures of the vapor in the chamber and the aluminum block near the grooves.

Heat is added to a short length of a chamber which is has a felt metal wick wrapped around the periphery which is saturated with ammonia. The generated vapor then condenses on the Gregorig grooves. The felt metal wick draws liquid out of the groove troughs and returns it to the heated section where it is vaporized. The chamber may be thought of as a heatpipe where the grooved aluminum block is its condenser section. Unlike the previous ground experiment, liquid is drawn off the grooves in a continuous manner which more accurately simulates operation of a flight version of HETI.

Assembly of the experimental setup shown in Figure 5-1 was nearly completed at the end of the Phase A contract. During Phase B, the assembly will be completed and the test will be performed with the grooves facing upward and grooves facing downward.

5.1-2 Preliminary Mechanical Design

Mechanical design of the experiment will commence in Phase B. This design effort will conform to aerospace industry practice and NASA requirements stipulated in References [12] and [13]. Only materials with a high resistance to stress corrosion cracking will be selected. For safety reasons, exposed corners, edges, and protrusions will be minimized in the design. Material properties used in the design process will be obtained from MIL-HDBK-5D. Required mass properties data will be generated by analysis and/or test.

5.1-3 Thermal Analysis

Detailed thermal analysis of the TCS and its support hardware will be performed early in Phase B. The thermal analysis on the TCS is intended to: (a) determine the transient radiator temperature response as a function of evaporator heat load and orbiter orientation; (b) calculate the degree of thermal coupling required between the CPL accumulator and radiator which permits reasonable control of CPL saturation temperature without a large

expenditure of accumulator heater power; (c) determine the lengths of the liquid transport line and accumulator outlet line which must be coupled to the radiator plate to provide the required degree of liquid subcooling; (d) compute heater power requirements for experiment electronics; and (e) provide pre-flight test temperature predictions. A detailed thermal model of the vapor chamber of the HETI will be developed in order to calculate the number of moles of non-condensible gas which should be contained in the gas reservoir. The amount of gas included should be able to block approximately one-third of the vapor chamber for each heatpipe when the CPL saturation temperature is 20°C. Determination of the required gas inventory will be performed using VCHPDA, a TRW-developed SINDA subroutine used to model variable conductance heatpipes.

Thermal analyses of support hardware such as multiplexers, logic circuits, and other command and data handling hardware are planned. The purpose of these analyses are to determine heater powers required to maintain these components above their minimum design temperatures and calculate their maximum expected temperatures. The result of this portion of Phase B is an integrated SINDA model comprising all components of the experiment.

5.1-4 Structural Analysis

Structural analyses will be performed during Phase B to arrive at required tube wall thicknesses, transition joint construction, and experiment response to Shuttle launch loads. The maximum internal pressure of the CPL, HETI, and radiator heatpipes which will be used in the structural design of these components is 4.13 MPa, which is the saturation pressure of the ammonia in the TCS corresponding to the Shuttle abort condition temperature of 80°C. The structural design will utilize standard aerospace industry design practices, including analytical solutions for simpler geometries, the ASME Boiler Code where appropriate, and detailed NASTRAN finite element for critical locations. No attempt will be made to constructed detailed NASTRAN models of the entire TCS due to the prohibitive expense incurred from the construction of a large number of detailed NASTRAN models. The result of the Phase B structural analysis effort will be a TCS structural design which will be qualified by proof pressure testing early in Phase C/D.

5.1-5 Support Electronics Design

Design of hardware and software for the experiment data acquisition and command/control systems is planned for Phase B. This work will include development of both CCGSE and CGSE. The expected outputs from this effort will

include: (1) drawings of the payload analog multiplexing circuit, relay control circuit, and control logic circuit; (2) drawings showing locations of all controllable hardware and instrumentation; (3) documents and drawings detailing electrical and physical interfaces between the payload and the SPOC avionics unit; (4) documents and drawings detailing interfaces between the CCGSE and CGSE; and (5) documents describing software for the CGSE.

5.1-6 TCS Breadboard Testing

A breadboard model of the TCS will be constructed in Phase B. This breadboard will include a CPL, an HETI, and a radiator plate with two heatpipes. The purpose of the breadboard is to verify thermal function of this integrated system of components prior to fabrication of flight hardware. This breadboard hardware may later be subject to structural qualification testing.

5.1-7 Preparation of Safety Documentation

Initial phases of the safety review process will commence in Phase B. The purposes of the safety review process are to determine hazardous aspects of the payload and GSE and implementing corrective measures and to assure compatibility of the payload with Orbiter interfaces. The Phase 0/1 review will include a safety plan, reliability and quality assurance plan, software development plan, and experiment development plan. The Phase 0/1 safety review will be conducted in the ninth month of Phase B. Potential hazards which will be examined for this payload include a pressurization of the TCS and use of a noxious working fluid (ammonia).

A TRW safety engineer will be assigned early in Phase B to serve as the project's single point of contact and authority for safety. The safety engineer will perform in-depth hazard analyses, prepares and maintains hazard reports and the flight and ground safety compliance data packages, and generally guides project design and test engineering personnel in satisfying the NSTS safety requirements. During environmental testing, a safety engineer is assigned to review and approve test procedures and provide safety surveillance during test conduct.

5.1-8 Phase B Cost and Schedule

The expected schedule and cost for Phase B of this IN-STEP program are summarized in Figures 5-2 and 5-3, respectively. The one-year contract duration mandates that many design activities proceed in parallel.

5.2 Phase C/D Activities

Phase C/D will include final detailed design, structural qualification of

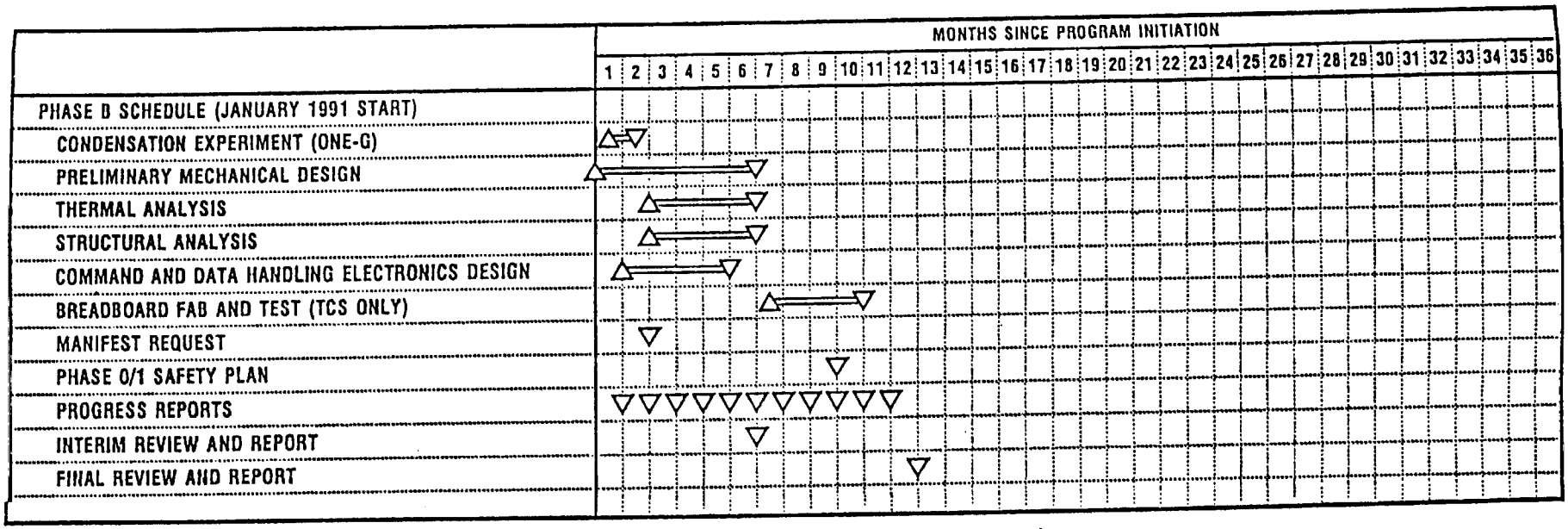

Figure 5-2. Phase B Schedule

	TASK	COST
1.	Condensation experiment	$ 7 K
2.	Mechanical design	$ 21 K
3.	Thermal analysis	$ 21 K
4.	Structural analysis	$ 32 K
5.	Support electronics design	$ 71 K
6.	TCS breadboard fab and test	$ 44 K
7.	Safety engineering	$ 31 K
8.	Project management, documentation, and travel	$ 107 K
	Total	$ 334 K

Figure 5-3. Expected Phase B Costs

the TCS components using proof and burst pressure testing, experiment fabrication and integration into the GAS-type canister, thermal vacuum testing, vibration and acoustic testing, EMI testing, and pre- and post-flight support activities. In addition to the activities described below, safety documentation will be provided and experiment manifesting procedures will occur.

5.2-1 Final Detailed Design

Final design drawings of the experiment and its GSE will be prepared within the first four months of Phase C/D. These final drawings will be reviewed by the Hitchhiker Office of GSFC prior to hardware fabrication. Mechanical interface drawings produced on this activity will be controlled by GSFC. Circuits and power distribution schematics for the experiment will also be provided to GSFC.

5.2-2 Structural Qualification

A Structural Integrity Verification Plan will be produced by TRW early in this phase. The TCS will be designed in accordance with NHB 1700.7B. The method chosen to verify structural integrity of the TCS, which would qualify as a pressure vessel, is a proof pressure and burst pressure test program. The test program will demonstrate that there are no permanent deformations or ultimate failures of the structure when loads are imposed on the structure such that every primary load-carrying member experiences a stress equal to a minimum of 1.25 times the limit stress. The limit stress is the highest stress produced by the design limit acceleration load factors. A portion of this activity will be preparation of a Fracture Control Implementation Plan. The purpose of this plan is to ensure that no catastrophic hazards to the STS or crew will result from initiation or propagation of flaws or cracks in customer structure during its mission lifetime, including fabrication, testing, and service life. The requirements for fracture control are usually satisfied by HH-G payloads without a Motorized Door Assembly (MDA), which this experiment will not possess.

5.2-3 Experiment Fabrication

The TCS for the experiment will be fabricated by TRW. It will utilize an all-welded construction. Radiographic inspection of all welds will be performed to ensure the structural integrity of the experiment. Command and data acquisition hardware for the experiment and GSE will be manufactured or purchased by TRW. In the event that command or data acquisition is available

from prior flight test programs as GFE, the equipment will be used to produce a program cost savings.

5.2-4 Experiment Integration Into HH-G Canister

Prior to qualification testing (thermal vacuum, thermal cycle, vibration, acoustic, and EMI), the experiment will be integrated into a dummy HH-G canister. After completion of testing at TRW, the experiment will be integrated into the flight GAS-type HH-G canister at GSFC. TRW will provide the required insulation materials and handling fixtures for the experiment.

5.2-5 Thermal Vacuum Testing

Upon fabrication of the experiment and integration into the HH-G canister, the experiment will undergo a thermal vacuum qualification test at TRW. The purpose of this test is to verify temperature predictions of the SINDA thermal math model for a wide range of CPL evaporator heater powers and environmental heat load conditions. The TCS will be able to operate in a gravity-assisted mode during theis test, so nearly isothermal operation of the CPL, HETI, and radiator heatpipes should result. Tape heaters on the top and sides of the canister will simulate solar, albedo, and earth IR heating. This test will examine heater duty cycles for the all thermally-controlled instrumentation and estimate cooldown times for the radiator.

5.2-6 Vibration, Acoustic, and EMI Qualification Testing

Vibration, acoustic, and electromagnetic interference (EMI) qualification testing of the integrated experiment and canister will be performed at TRW. The payload must survive the random vibration, acoustic, and EMI environments stipulated in [12].

5.2-7 Delivery and Integration

During this phase of the contract, TRW will assist in pre-flight testing of the experiment and integration into the Orbiter. The pre-flight testing will include verification of Orbiter interfaces.

5.2-8 Flight Operations and Support

Prior to flight operations, operational plans and procedures for flight operation will be established. During flight operations which will be conducted at GSFC, TRW will provide test engineers to monitor telemetry, implement the command plan, and make necessary changes in the command plan. A tentative test plan is shown in Figure 5-4. Upon completion of the mission, TRW will safe the payload and de-integrate the payload from the HH-G canister. A final report will be prepared, discussing microgravity performance of the

TEST NO.	HEATER POWER LEVEL (WATTS) / DURATION (MINUTES)				TOTAL TEST TIME (MIN)	OBJECTIVE
	EVAPORATOR 1	EVAPORATOR 2	INLET 1	INLET 2		
1	250/30	250/30	0/30	0/30	30	(Up to 367W ea.) Response to instant power
2A	250/40	125/40	0/40	0/40	40	Test response to differential heating
2B	125/40	250/40	0/40	0/40	40	
3A	75/60	75/60	0/60	0/60	60	Low power limit
3B	50/60	50/60	0/60	0/60	60	
3C	25/60	25/60	0/60	0/60	60	
4A	250/40	0/20, 250/20	0/40	0/40	40	Heat sharing
4B	0/20, 250/20	250/40	0/40	0/40	40	
5A	250/40	250/25, 0/15	0/15, 25/10, 0/15	0/40	40	Induce deprime
5B	250/25, 0/15	250/40	0/40	0/15, 25/10, 0/15	40	
6A	250/20, 125/20	250/20, 125/20	0/40	0/40	40	Power step down
6B	250/40	250/20, 125/20	0/40	0/40	40	
6C	250/20, 125/20	250/40	0/40	0/40	40	
7A	125/20, 200/20, 70/20	125/20, 200/20, 270/20	0/60	0/60	60	Power step up
7B	125/60	125/20, 200/20, 270/20	0/60	0/60	60	
7C	125/20, 200/20, 270/20	125/60	0/60	0/60	60	
8A	300/25	300/25	0/25	0/25	25	High power response
8B	350/20	350/20	0/20	0/20	20	
8C	250/10, 300/10, 350/10	250/10, 300/10, 350/10	0/30	0/30	30	
9A	125/70	125/70	0/70	0/70	70	Release NCG (NCG test start up w/NG)
9B	125/40	125/40	0/40	0/40	40	

Figure 5-4. Experiment Flight Test Plan

integrated two-phase TCS.

5.2-9 Phase C/D Cost and Schedule

The expected schedule and cost for the three-year duration of Phase C/D of this IN-STEP program are summarized in Figures 5-5 and 5-6, respectively. The launch date shown in Figure 5-5 assumes an early manifesting for the experiment.

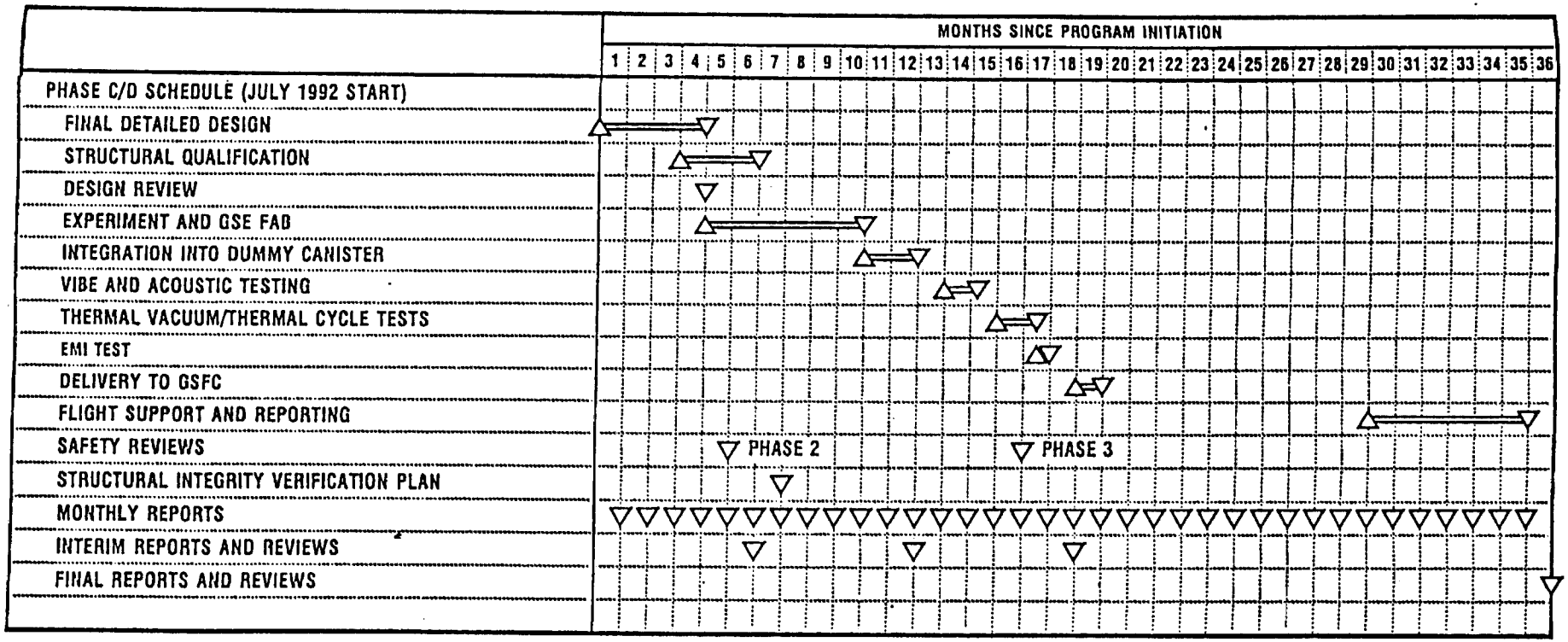

Figure 5-5. Phase C/D Schedule

	TASK	COST
1.	Final detailed design	$ 192 K
2.	TCS fabrication	$ 69 K
3.	Support electronics fabrication	$ 136 K
4.	Thermal vacuum testing	$ 49 K
5.	Thermal cycle testing	$ 17 K
6.	Vibration testing	$ 32 K
7.	Acoustic testing	$ 18 K
8.	EMI testing	$ 43 K
9.	Proof pressure testing	$ 26 K
10.	Safety engineering	$ 79 K
11.	Pre-flight activities	$ 71 K
12.	Flight operations	$ 55 K
13.	Post-flight analysis	$ 31 K
14.	Project management, documentation, and travel	$ 254 K
	Total	$1072 K

Figure 5-6. Expected Phase C/D Costs

6. SUMMARY AND CONCLUSIONS

The purpose of this flight experiment is to determine operational characteristics of a two-phase thermal control system (TCS) consisting of a capillary pumped loop (CPL), a heatpipe radiator, and a High Efficiency Thermal Interface (HETI) which couples these two components. This experiment will also obtain fundamental data regarding condensation and evaporation heat transfer processes in microgravity conditions and will assess the thermal and hydrodynamic behavior of CPL reservoirs. This integrated thermal control system is applicable to a wide range of NASA and DoD spacecraft with heat dissipations approaching or exceeding 5 kW.

The experiment draws extensively upon prior development of CPLs and the HETI by NASA and the Air Force. Large CPL engineering models with and without mechanical pump assists have been designed, fabricated, and tested extensively. Two small-scale CPL flight experiments have been flown successfully on the STS Get-Away Special and Hitchhiker-G carriers. Heatpipe radiators have demonstrated very successful operation in microgravity. A microgravity flight experiment is required to verify performance of this thermal control system because liquid flow in the HETI is dominated by gravitational forces during ground testing.

Conceptual design of this experiment was completed in Phase A. The work completed in this phase includes: (1) an experiment layout; (2) a preliminary test plan; (3) selection of the Hitchhiker-G as the required carrier; (4) the outline, schedule, and expected cost for Phase B; and (5) partial fabrication of a ground experiment intended to validate a mathematical model of condensation on the Gregorig-grooved surfaces in the HETI. The anticipated cost for a one-year duration Phase B contract for this experiment is $334K. At the conclusion of Phase B, the experiment design will have matured to a near-Critical Design Review stage. The expected cost for the three-year Phase C/D program is $1072K. Cost savings can be realized if CPL hardware or ground support equipment from previous flight experiments may be utilized in this contract. Based on previous testing of individual components of this experiment, as well as the flight heritage of the command and data acquisition subsystem design, we expect no technology, cost, or schedule "show-stoppers" to arise during the development of this experiment.

REFERENCES

1) Mertesdorf, S.J., Pohner, J.A., Herold, L.M., and Busby, M.S., "High Power Spacecraft Thermal Management, Task 2. Technology Assessment, Final Report," AFWAL-TR-2121, Vol. II, April 1987.

2) Presler, A.F., et. al., "Liquid Droplet Radiator Program at the NASA Lewis Research Center," ASME 86-HT-15, June 1986.

3) Knapp, K., "Study of Moving Belt Radiators for Heat Rejection in Space," AFRPL-TR-84-001, January 1984.

4) Ponnappan, R., et. al., "Conceptual Design of a 1 m Long 'Roll Out Fin' Type Expandable Space Radiator," AIAA-86-1323, June 1986.

5) Kroliczek, E.J., Ku, J., and Ollendorf, S., "Design, Development, and Test of a Capillary Pump Loop Heat Pipe," AIAA-84-1720, June 1984.

6) Ku, J., Kroliczek, E.J., Taylor, W.J., and McIntosh, R., "Functional and Performance Test of Two Capillary Pumped Loop Engineereing Models," AIAA-86-1248, June 1986.

7) Gregorig, von Romano, "Hautkondensation an Feingewellten Oberflachen bei Berucksichtigung der Oberfachenspannungen," Zeitschrift fur Angewandte Mathematik und Physik, Vol. 5, 36-49 (1954).

8) Eninger, J.E., "High Power Spacecraft Thermal Management, Task 5. High Efficiency Interface for Advanced Radiators, Draft Final Test Report," TRW Report No. 44104-063, May 1988.

9) "IN-STEP 88 Workshop Proceedings," NASA Office of Aeronautics and Space Technology, December 1988.

10) Ku, J., Kroliczek, E.J., Butler, D., Schweikart, R.B., and McIntosh, R., "Capillary Pumped Loop GAS and Hitchhiker Flight Experiments," AIAA-86-1249, June 1986.

11) "Carriers for In-Space Technology Experiments," NASA Goddard Space Flight Center, prepared by OAO Corporation (1988).

12) "Hitchhiker Shuttle Payload of Opportunity Carrier Customer Accomodations and Requirements Specification," NASA Goddard Space Flight Center, HHG-730-1503-04, July 1988.

13) "Safety Policy and Requirements for Payloads Using the Space Transportation System," NASA Johnson Space Center, January 1989.